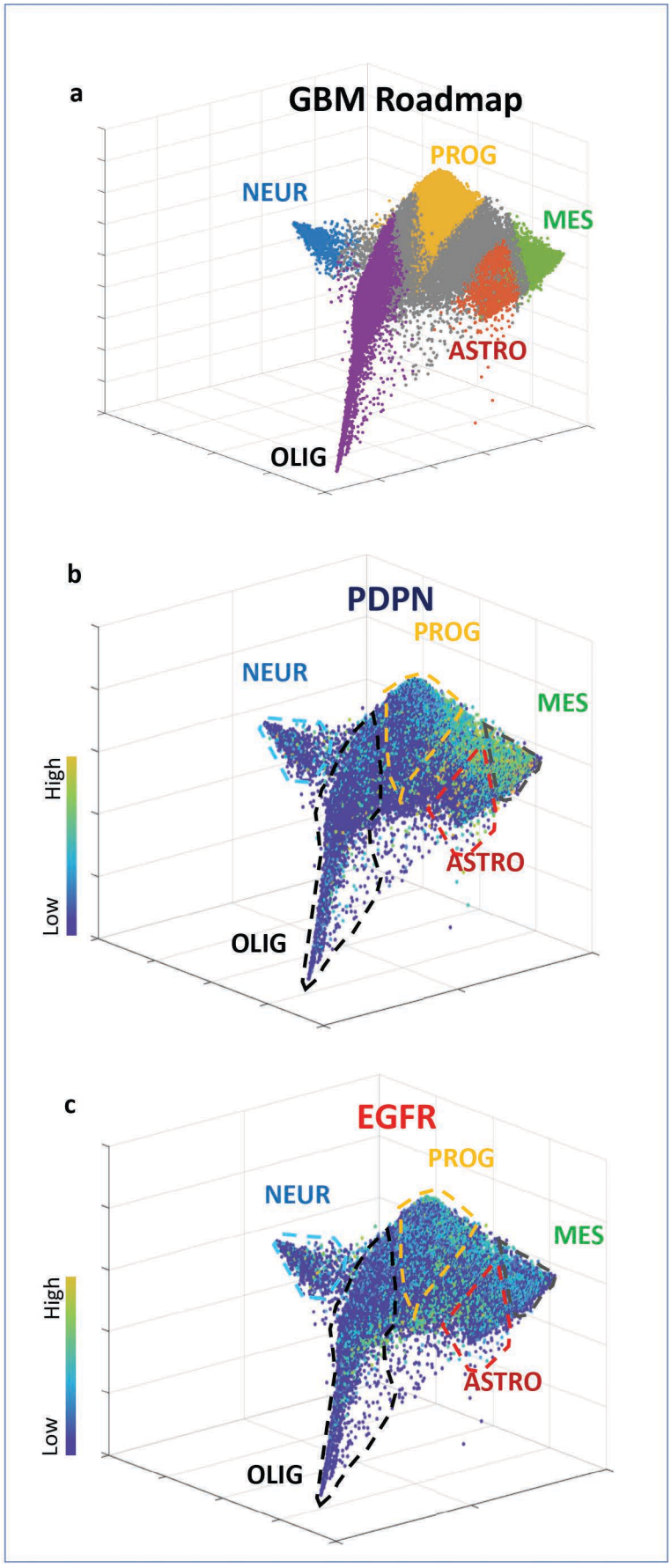

Supplementary information - Figure S1

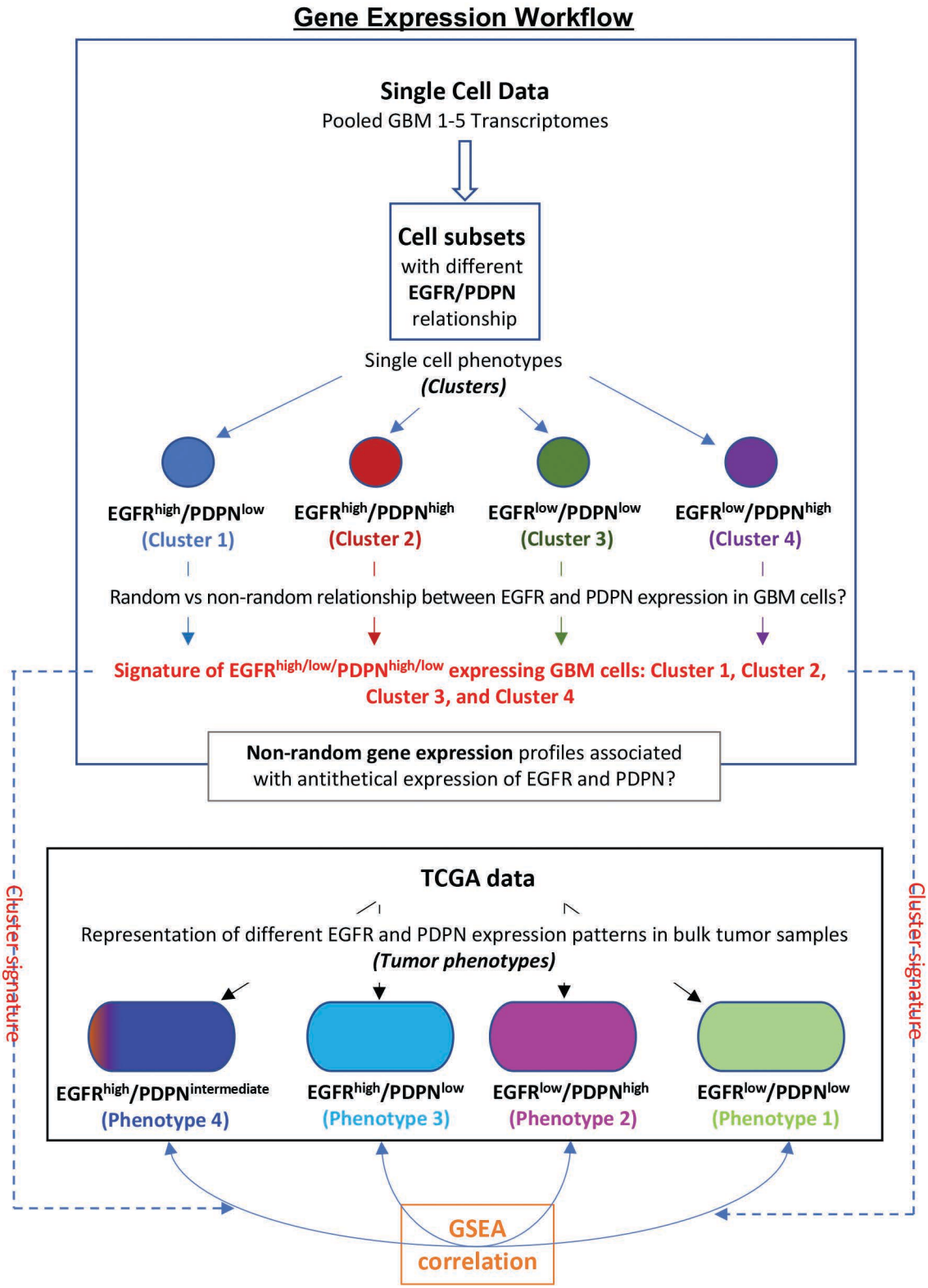

Supplementary information - Figure S2

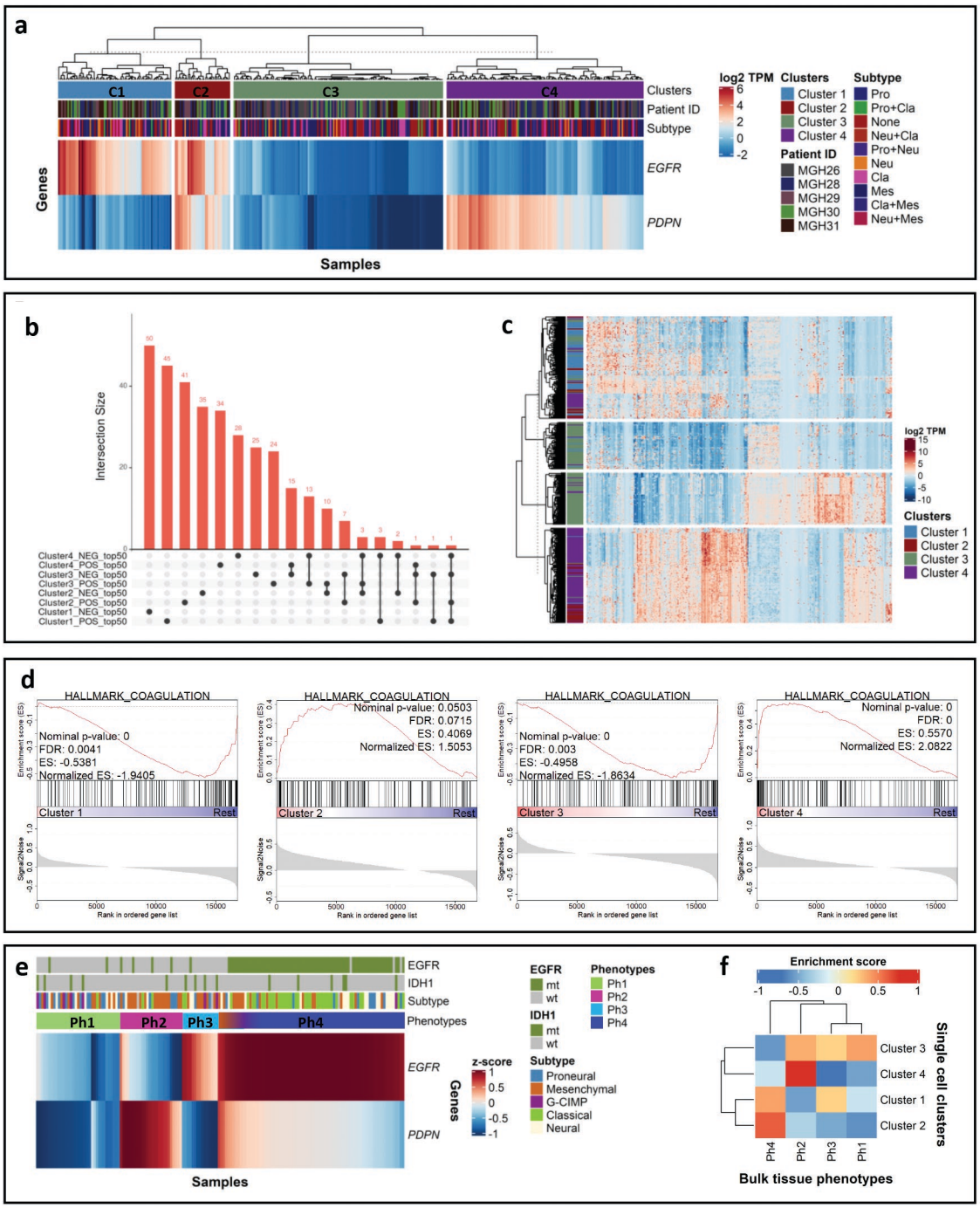

Supplementary information - Figure S3

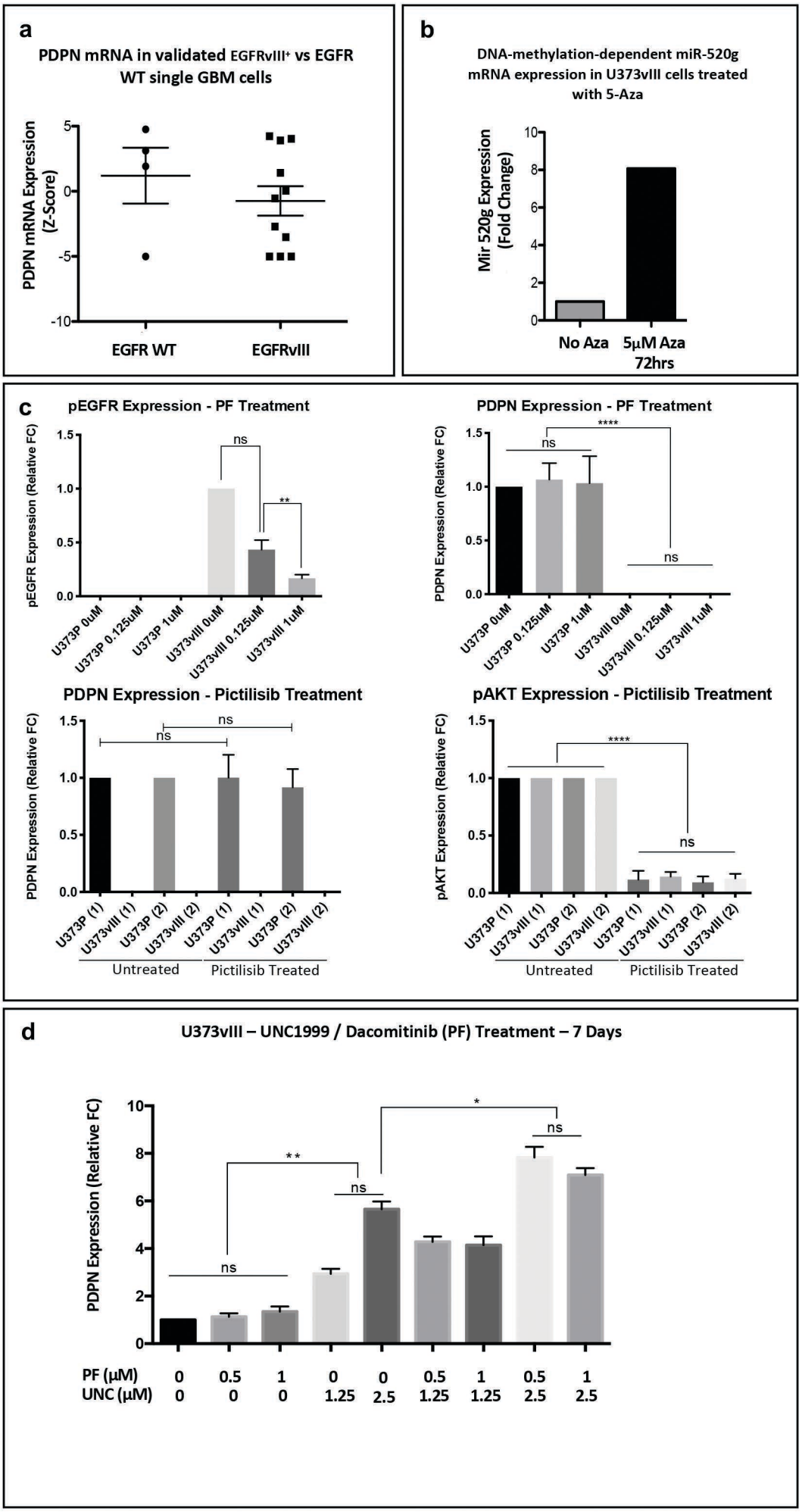

Supplementary Figure S4

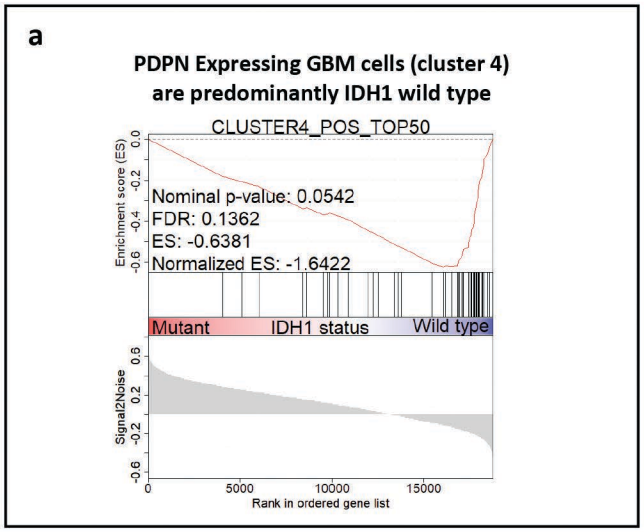

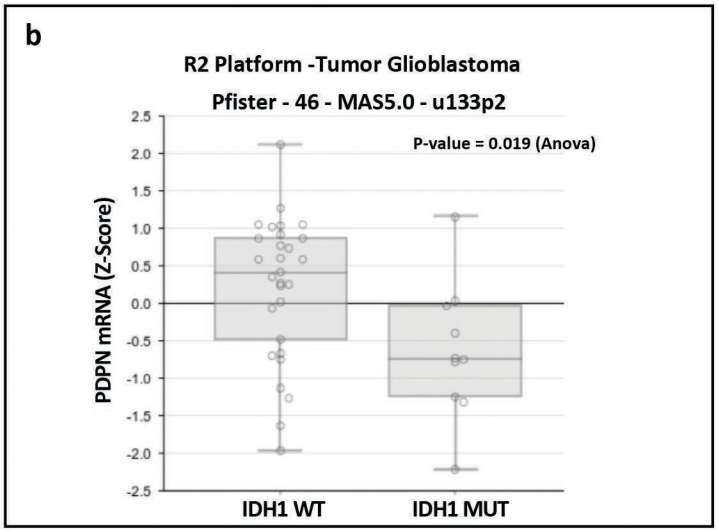

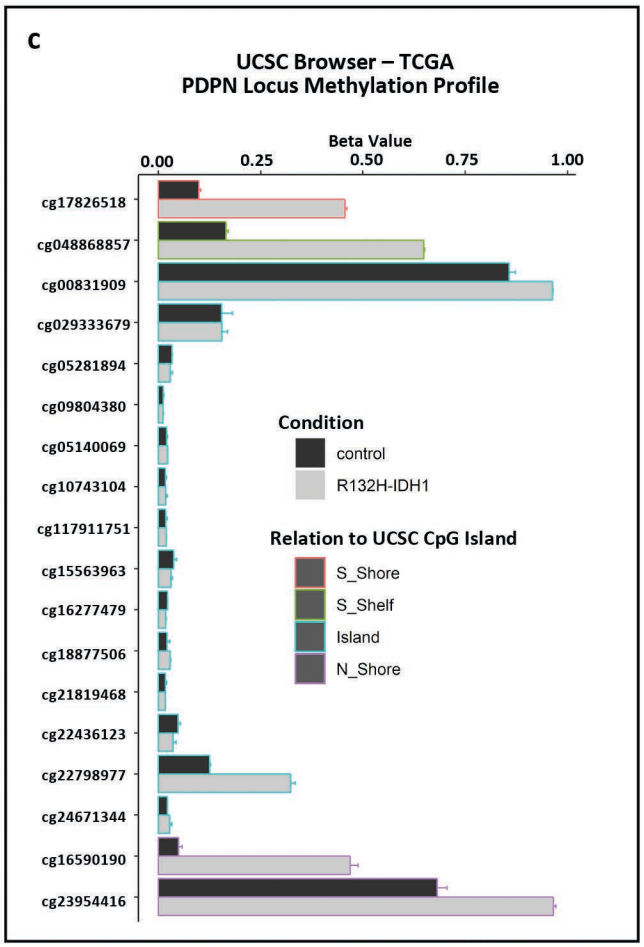

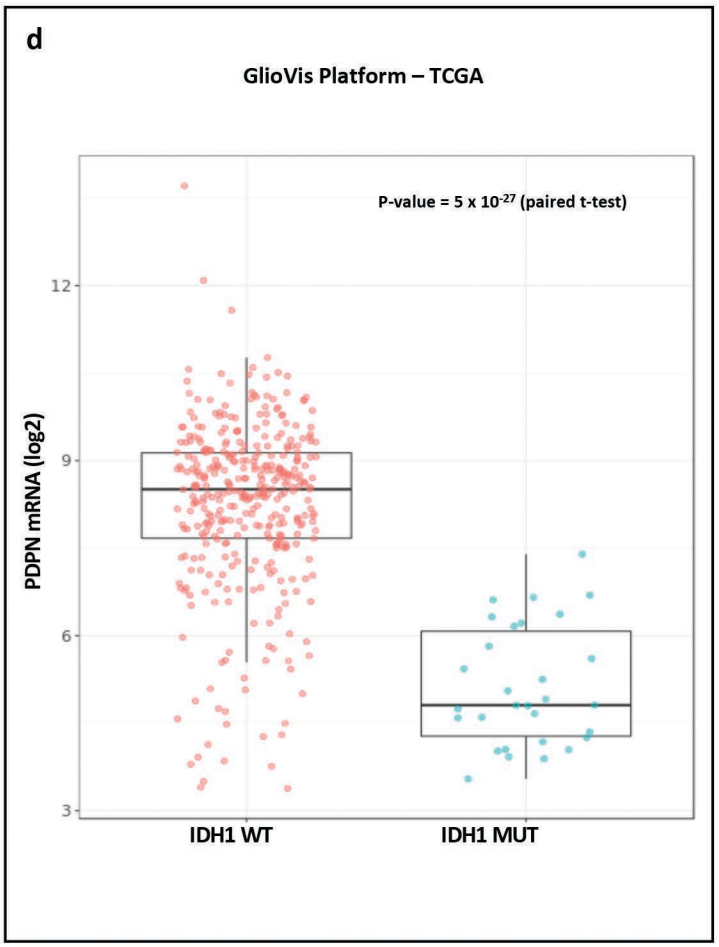

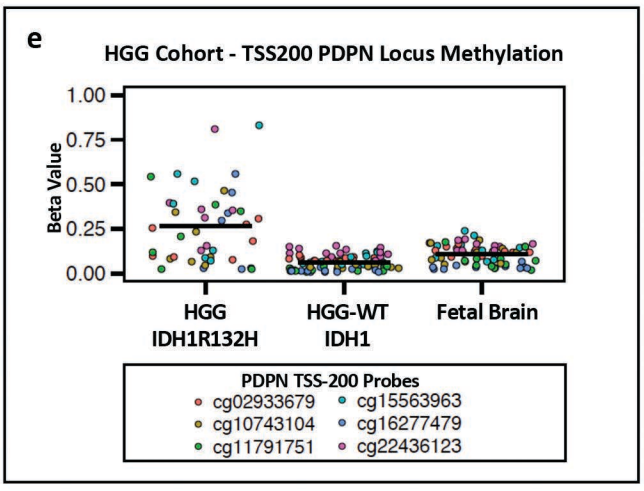

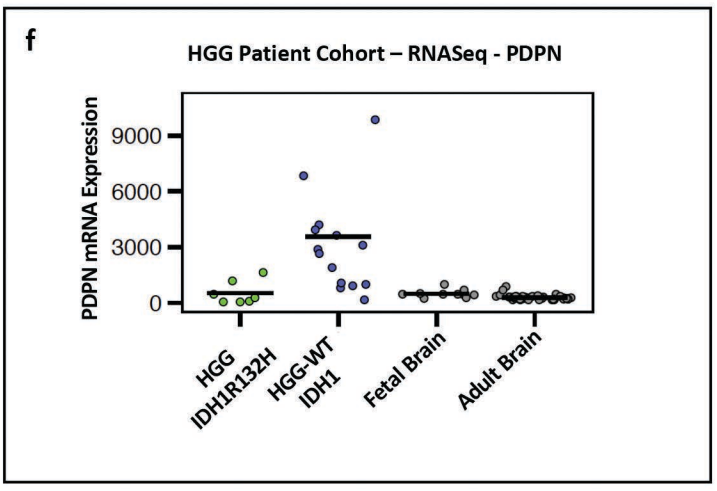

Supplementary information - Figure S5

Circulating TF immunoreactivity in plasma of patients with glioblastoma (GBM)

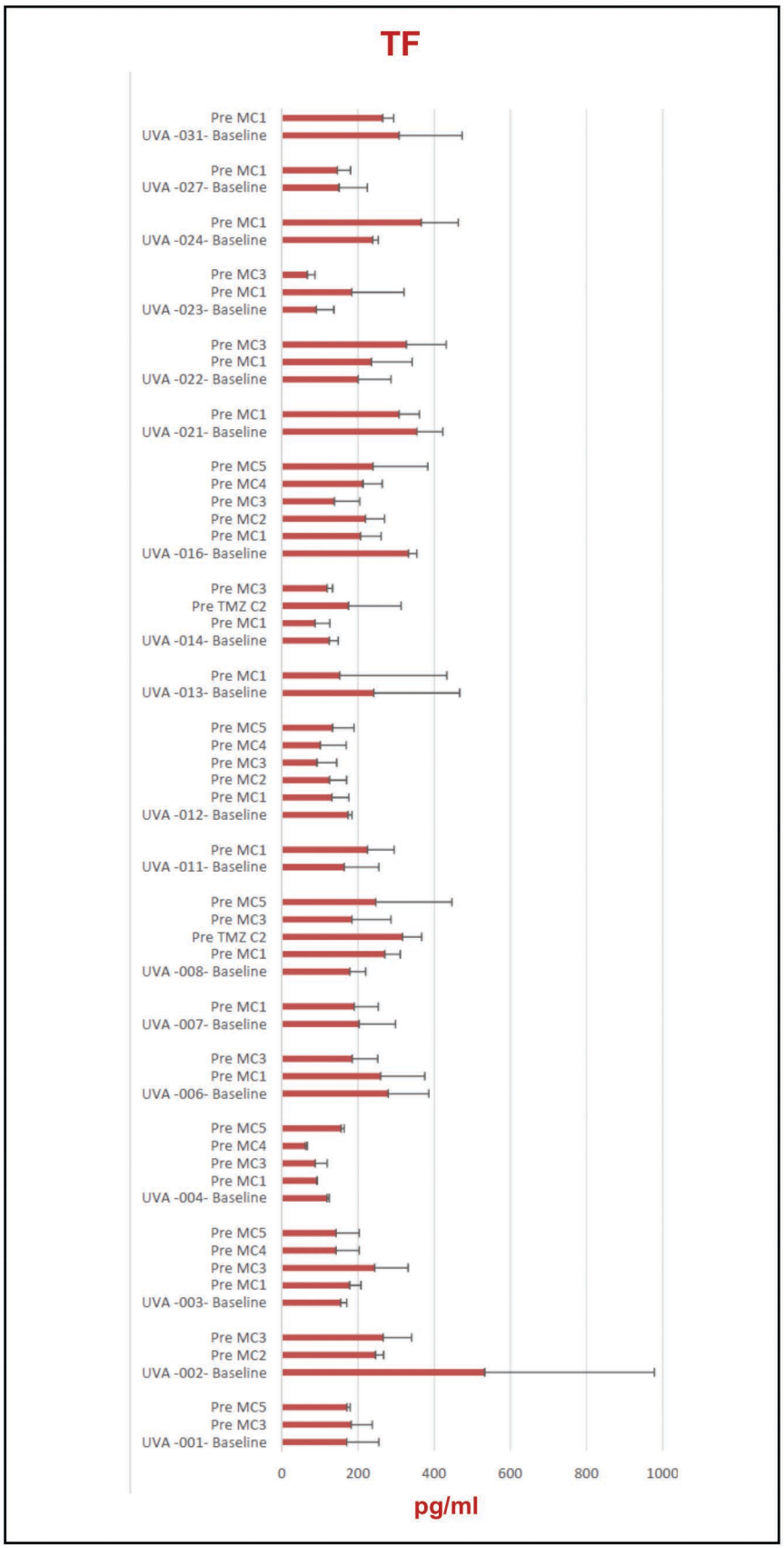

Supplementary Figure S6

a GSEA Analysis of PDPN/EZH2 Correlations within the Sigle Cell Dataset (Patel et al. 2014)

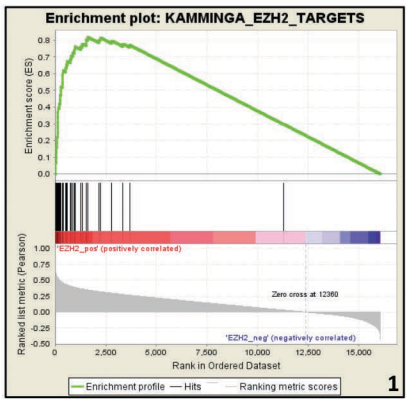

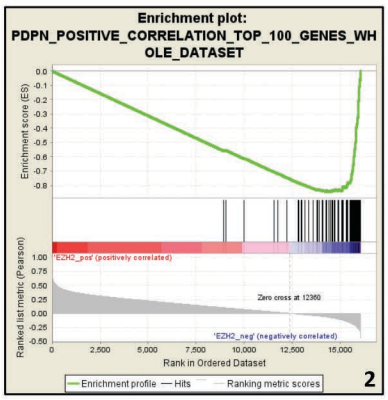

1. Curated EZH2 upregulated genes are positively correlated with EZH2 expression across the whole data set. FDR= 0.013

2.Genes positively correlated with PDPN are negatively correlated with EZH2 expression. FDR= 0.015

b U373 PT EVs. Immunogold Double stained: PDPN 10nm / CD63 5nm. Direct Magnification 30000X FEMR

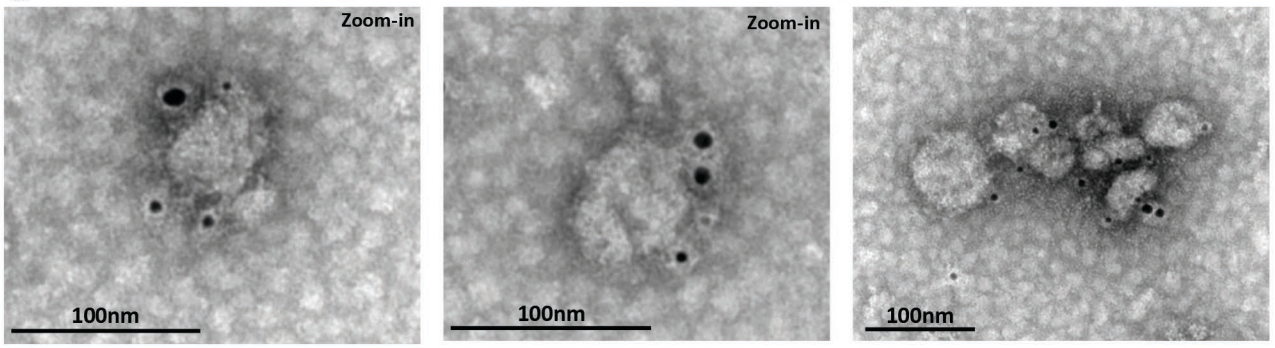

c

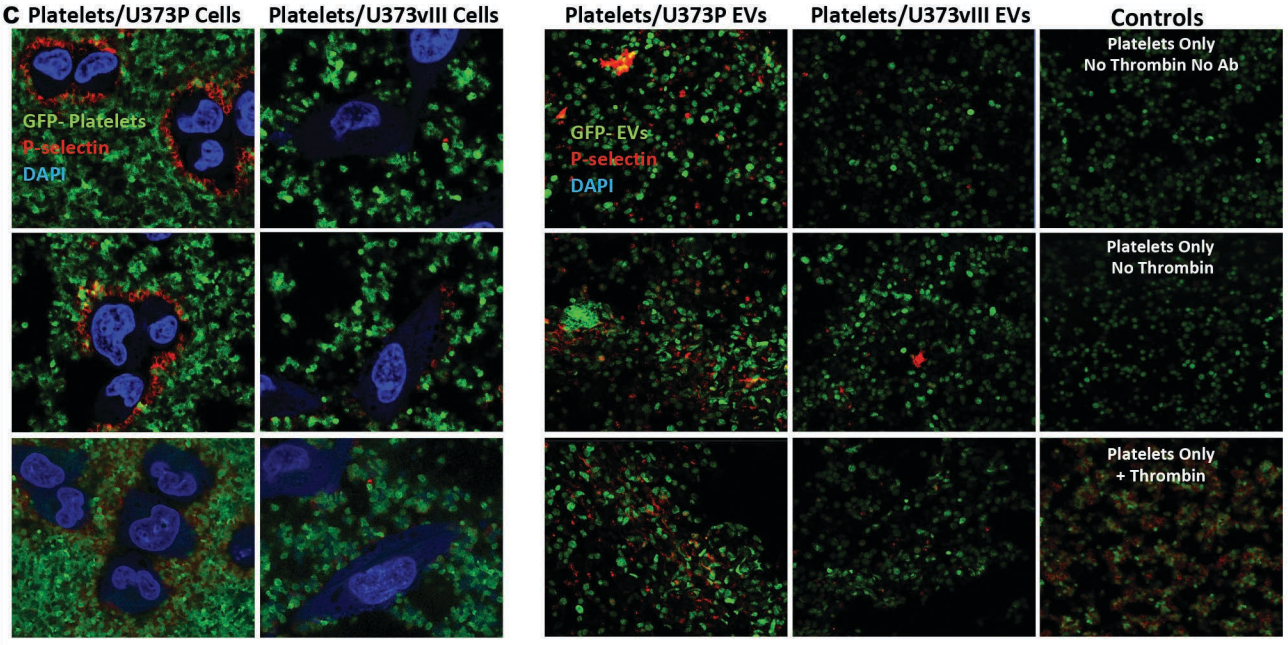

Supplementary Figure S7

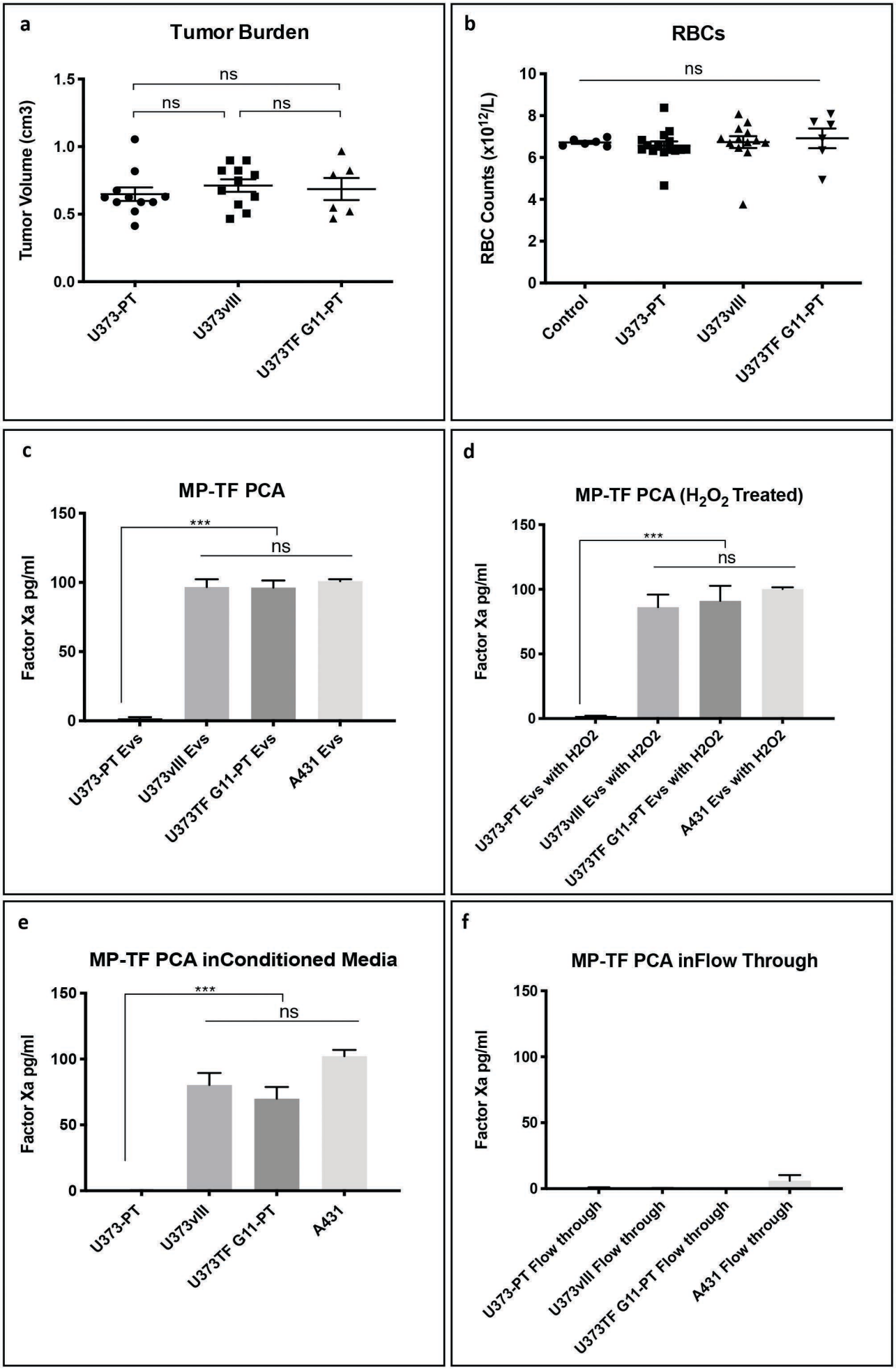

Supplementary Figure S8

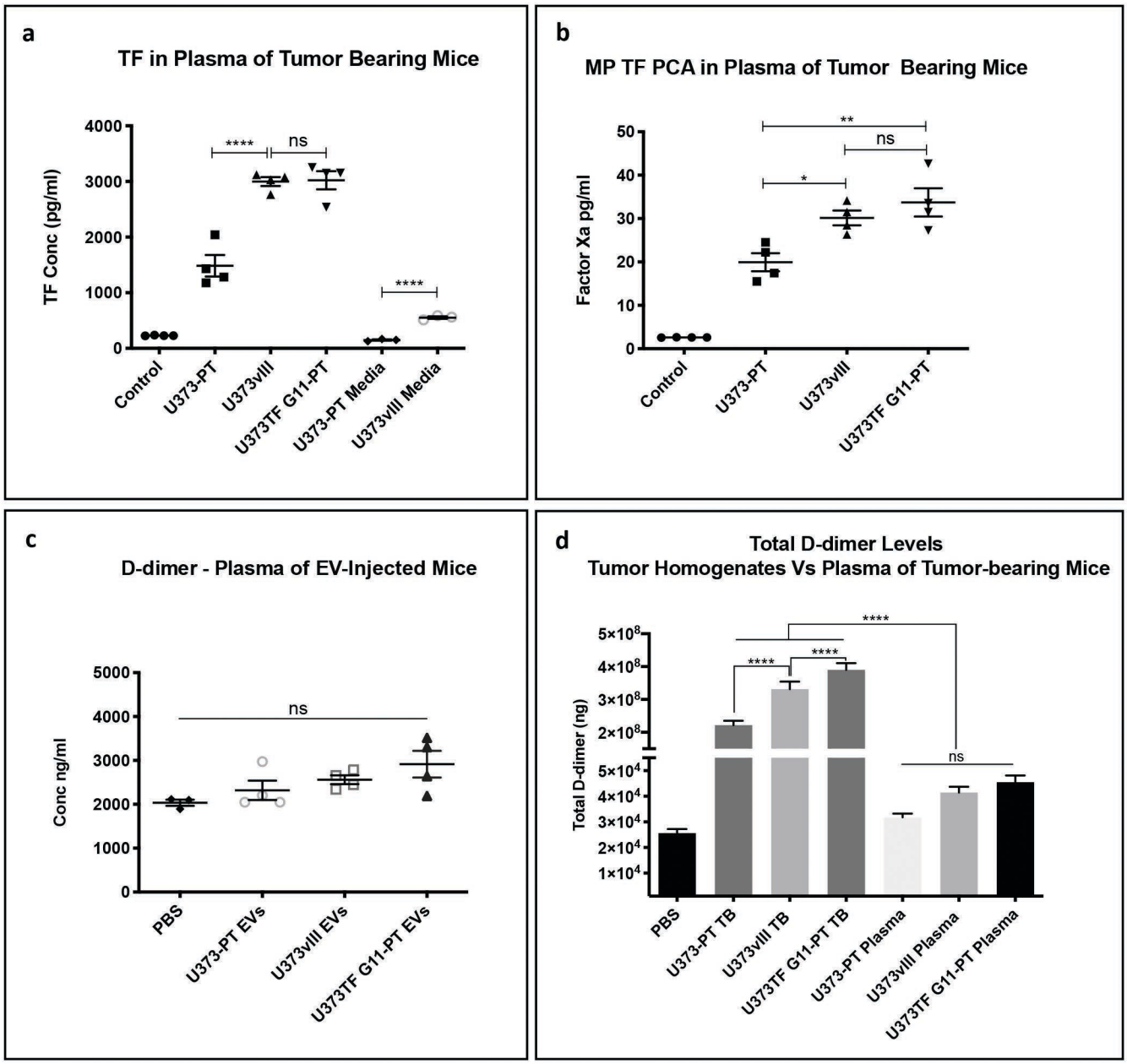

Supplementary Figure S9

Top 50 Gene Signatures of Clusters 1-4

CLUSTER 1		CLUSTER 2		CLUSTER 2		CLUSTER 4	
Cluster1_POS_top50	Cluster1_NEG_top50	Cluster2_POS_top50	Cluster2_NEG_top50	Cluster3_POS_top50	Cluster3_NEG_top50	Cluster4_POS_top50	Cluster4_NEG_top50
EGFR	SERPINE1	EGFR	ACTRT1	MAGEC2	DNAJC15	PDPN	RPS23
C2orf80	CCR7	PDZD2	MAGEB2	TMSB15A	BST2	CD68	RPLP1
PLPPR1	LYPD3	MEIS1	RPL3	MAGEA12	PGAM2	SERPING1	MCM10
LINC00266-1	PSMD3	AQP4	PHLDB2	ITIH6	SDC4	EFEMP1	RPL37A
OLIG1	LOXL2	PDPN	RPLP2	CD163L1	NRCAM	GFPT2	CD163L1
LMO1	ITGB5	ALDH1L1	NDUFB2	GALNT14	ATP13A4	CHI3L1	GPR153
ARL4A	HSPB3	LGI1	RNF144A	KLRC2	AGT	CCN1	PCDH15
GALR1	S100A4	ARHGAP1	RPL37A	MAGEB2	EGFR	EFNA1	EGFR
SHD	STC1	GRIA1	RPL10	RPL35	C4orf47	SULF1	RPL35
RPS4Y1	LCTL	BST2	SULT2A1	RPS20	ZNF516	CAV1	CENPV
CD82	AZIN2	TIMP3	UGT1A5	RPL27	PLAAT4	C1R	HELLS
PCDH17	GLIPR1	ATP13A4	MBNL3	RPL12	GADD45B	GAP43	MAGEA12
LINC01546	NR4A2	PTEN	OR5B3	CSAG1	EFEMP1	PCSK1	MAGEC2
SCG3	IL13RA1	ATP1A2	PRRT4	ADCK5	CHI3L1	PLA2G5	SULT2A1
CRISPLD2	C8orf88	RBP1	PTPA	MCM10	SERPINB6	SDC4	RPL27
RBP7	CTSH	ATP1B2	OR52E4	RPL21	DPF3	VWA5A	RPL23A
PTPRO	TGFBI	SLITRK5	TMEM98	CDC6	SPP1	EMP1	RPL21P7
ACTA1	S100A3	ALDOC	OR8G1	SIX6	TCEAL5	SPOCD1	RPS27L
APOD	DDR2	KLHL4	FBXL22	RPL26	RCAN2	TGFB2	ATP5MPL
NKAIN4	PRELID2	ADAMTS6	NUBP2	PHLDA2	SPOCD1	IFI35	RPL39
BEX1	SLC43A1	MBOAT2	PHLDA2	RPL39	SPARCL1	BCL6	RPL4
FSCN1	MGST1	RSRP1	RARG	RPL35A	CTSK	TCIM	TMSB15A
TSPAN7	OSR2	PCDHB11	NECAB2	MSC	DDX3Y	GPC1	RPS16
DLL1	SLC7A3	PRR13	DLX5	FGF13	NME5	CLU	LAMA1
LANCL2	ERICH2	KLF9	KLRC2	RPL32	SLC25A18	EFEMP2	HMGN2
TLE2	ITGA5	SMARCC2	COL2A1	SLFN11	PLA2G5	SRPX2	NPM1
OCIAD2	POLE4	SLC15A2	SHISAL1	C14orf39	ZBTB20	NAMPT	TMEM98
ATCAY	CTSC	SLC1A3	RPS11	NQO1	TGFB2	ELMOD1	SOX10
MOG	ZCCHC12	COLGALT2	C10orf120	OR5G5P	TMBIM1	C1S	STMN1
NCALD	SLC7A8	OLFM2	MSC	RPL23A	CAMK2N1	PPFIA2	BUB1B
FAIM2	TANGO2	PHYHIPL	KCNAB3	BUB1B	C1R	SOD2	CDC6
TSC22D4	OAF	C19orf18	GDPD3	SFRP2	PCDHB11	MAOB	FANCI
KCNQ2	BLVRB	SLC30A4	SLFN11	TMA7	CCDC152	TMBIM1	HMGB1
GPR37L1	SLC39A12	RAB3D	FCGR2B	RPL7	CCN1	HS3ST3B1	RPS21
TENM1	CALCB	S1PR2	ENAM	RPL19	SCN3A	CADPS	RAB33A
TMEM233	NABP1	SNX27	RPL7	KRTAP13-4	C19orf18	CHI3L2	COL9A3
FAM222A	SLC39A14	ZFHX4	FCRLA	HMGB2	ALDOC	CLEC2B	RPL26
NFIX	CNN1	AASS	ITIH6	NPM1	GAP43	UBD	OLIG1
CRIP1	ANXA1	ABCD2	OST4	HBQ1	DHRS3	TAGLN	KLRC2
POSTN	RGS10	UBE2B	GALNT14	RPL37A	ABCA1	BHLHE40	RPS6
CNTN1	GEM	SRGAP2C	RPL30	TAAR1	RNF180	SPP1	RPL21
NKD1	TFPI2	NFIA	LENG1	FBXL22	TCIM	PNPLA4	KLRC4
SOX8	ARHGDIB	TMED9	MOGAT1	RPS27	IRF9	TAGLN2	RPS17
OR6C1	ALPL	F11R	TMSB10	FCRLA	CD68	CES1	EMP2
SLAIN1	ST8SIA4	ARAP2	ATP5F1E	MYCNOS	ADM	S1PR1	ZDHHC22
PRELID3B	NRP2	RNF180	OR10A2	NID2	SERPING1	PGM2L1	LINC01546
HLA-F	C9orf50	KIF13B	LAYN	RPL29	IRS2	MAN1C1	TM4SF1
INSYN2A	A2M	ITGB8	RPL3L	NR0B1	ZFP36	DHRS3	MTRNR2L1
RTN1	LDLR	CCDC152	MAGEC2	RPL14	FOSB	MMP7	MTAP
DNAJC15	MICA	SLC35A4	ADCK5	SH3KBP1	PDPN	GBP2	APOD

Supplementary information - Table S1

Table 2 Hallmark Coagulation
(https://www.gseamsigdb.org/gsea/msigdb/cards/HALLMARK_COAGULATION)

Original Member	NCBI (Entrez)	Gene Symbol	Gene Description
A2M	2	A2M	alpha-2-macroglobulin
ACOX2	8309	ACOX2	acyl-CoA oxidase 2
ADAM9	8754	ADAM9	ADAM metallopeptidase domain 9
ANG	283	ANG	angiogenin
ANXA1	301	ANXA1	annexin A1
APOA1	335	APOA1	apolipoprotein A1
APOC1	341	APOC1	apolipoprotein C1
APOC2	344	APOC2	apolipoprotein C2
APOC3	345	APOC3	apolipoprotein C3
ARF4	378	ARF4	ADP ribosylation factor 4
BMP1	649	BMP1	bone morphogenetic protein 1
C1QA	712	C1QA	complement C1q A chain
C1R	715	C1R	complement C1r
C1S	716	C1S	complement C1s
C2	717	C2	complement C2
C3	718	C3	complement C3
C8A	731	C8A	complement C8 alpha chain
C8B	732	C8B	complement C8 beta chain
C8G	733	C8G	complement C8 gamma chain
C9	735	C9	complement C9
CAPN2	824	CAPN2	calpain 2
CAPN5	726	CAPN5	calpain 5
CASP9	842	CASP9	caspase 9
CD9	928	CD9	CD9 molecule
CFB	629	CFB	complement factor B
CFD	1675	CFD	complement factor D
CFH	3075	CFH	complement factor H
CFI	3426	CFI	complement factor I
CLU	1191	CLU	clusterin
COMP	1311	COMP	cartilage oligomeric matrix protein
CPB2	1361	CPB2	carboxypeptidase B2
CPN1	1369	CPN1	carboxypeptidase N subunit 1
CRIP2	1397	CRIP2	cysteine rich protein 2
CSRP1	1465	CSRP1	cysteine and glycine rich protein 1
CTSB	1508	CTSB	cathepsin B
CTSE	1510	CTSE	cathepsin E
CTSH	1512	CTSH	cathepsin H
CTSK	1513	CTSK	cathepsin K
CTSL2	1515	CTSV	cathepsin V
CTSO	1519	CTSO	cathepsin O
DCT	1638	DCT	dopachrome tautomerase
DPP4	1803	DPP4	dipeptidyl peptidase 4

DUSP14	11072	DUSP14	dual specificity phosphatase 14
DUSP6	1848	DUSP6	dual specificity phosphatase 6
F10	2159	F10	coagulation factor X
F11	2160	F11	coagulation factor XI
F12	2161	F12	coagulation factor XII
F13B	2165	F13B	coagulation factor XIII B chain
F2	2147	F2	coagulation factor II, thrombin
F2RL2	2151	F2RL2	coagulation factor II thrombin receptor
F3	2152	F3	coagulation factor III, tissue factor
F8	2157	F8	coagulation factor VIII
F9	2158	F9	coagulation factor IX
FBN1	2200	FBN1	fibrillin 1
FGA	2243	FGA	fibrinogen alpha chain
FGG	2266	FGG	fibrinogen gamma chain
FN1	2335	FN1	fibronectin 1
FURIN	5045	FURIN	furin,
FYN	2534	FYN	FYN proto-oncogene, Src family tyrosine kin.
GDA	9615	GDA	guanine deaminase
GNB2	2783	GNB2	G protein subunit beta 2
GNG12	55970	GNG12	G protein subunit gamma 12
GP1BA	2811	GP1BA	glycoprotein Ib platelet subunit alpha
GP9	2815	GP9	glycoprotein IX platelet
GSN	2934	GSN	gelsolin
HMGCS2	3158	HMGCS2	3-hydroxy-3-methylglutaryl-CoA synthase
HNF4A	3172	HNF4A	hepatocyte nuclear factor 4 alpha
HPN	3249	HPN	hepsin
HRG	3273	HRG	histidine rich glycoprotein
HTRA1	5654	HTRA1	HtrA serine peptidase 1
ISCU	23479	ISCU	iron-sulfur cluster assembly enzyme
ITGA2	3673	ITGA2	integrin subunit alpha 2
ITGB3	3690	ITGB3	integrin subunit beta 3
ITIH1	3697	ITIH1	inter-alpha-trypsin inhibitor heavy chain
KLF7	8609	KLF7	Kruppel like factor 7
KLK8	11202	KLK8	kallikrein related peptidase 8
KLKB1	3818	KLKB1	kallikrein B1
LAMP2	3920	LAMP2	lysosomal associated membrane protein 2
LEFTY2	7044	LEFTY2	left-right determination factor 2
LGMN	5641	LGMN	legumain
LRP1	4035	LRP1	LDL receptor related protein 1
LTA4H	4048	LTA4H	leukotriene A4 hydrolase
MAFF	23764	MAFF	MAF bZIP transcription factor F
MASP2	10747	MASP2	mannan binding lectin serine peptidase 2
MBL2	4153	MBL2	mannose binding lectin 2
MEP1A	4224	MEP1A	meprin A subunit alpha
MMP1	4312	MMP1	matrix metallopeptidase 1

MMP10	4319	MMP10	matrix metallopeptidase 10
MMP11	4320	MMP11	matrix metallopeptidase 11
MMP14	4323	MMP14	matrix metallopeptidase 14
MMP15	4324	MMP15	matrix metallopeptidase 15
MMP2	4313	MMP2	matrix metallopeptidase 2
MMP3	4314	MMP3	matrix metallopeptidase 3
MMP7	4316	MMP7	matrix metallopeptidase 7
MMP8	4317	MMP8	matrix metallopeptidase 8
MMP9	4318	MMP9	matrix metallopeptidase 9
MSRB2	22921	MSRB2	methionine sulfoxide reductase B2
MST1	4485	MST1	macrophage stimulating 1
OLR1	4973	OLR1	oxidized low density lipoprotein receptor
P2RY1	5028	P2RY1	purinergic receptor P2Y1
PDGFB	5155	PDGFB	platelet derived growth factor subunit B...
PECAM1	5175	PECAM1	platelet and endothelial cell adhesion molecule
PEF1	553115	PEF1	penta-EF-hand domain containing 1
PF4	5196	PF4	platelet factor 4
PGCP	10404	CPQ	carboxypeptidase Q
PLAT	5327	PLAT	plasminogen activator, tissue type
PLAU	5328	PLAU	plasminogen activator, urokinase
PLEK	5341	PLEK	pleckstrin
PLG	5340	PLG	plasminogen
PREP	5550	PREP	prolyl endopeptidase
PROC	5624	PROC	protein C, inactivator of coagulation factor
PROS1	5627	PROS1	protein S
PROZ	8858	PROZ	protein Z, vitamin K dependent
PRSS23	11098	PRSS23	serine protease 23
RABIF	5877	RABIF	RAB interacting factor
RAC1	5879	RAC1	Rac family small GTPase 1
RAPGEF3	10411	RAPGEF3	Rap guanine nucleotide exchange factor 3...
RGN	9104	RGN	regucalcin
S100A1	6271	S100A1	S100 calcium binding protein A1
S100A13	6284	S100A13	S100 calcium binding protein A13
SERPINA1	5265	SERPINA1	serpin family A member 1
SERPINB2	5055	SERPINB2	serpin family B member 2
SERPINC1	462	SERPINC1	serpin family C member 1
SERPINE1	5054	SERPINE1	serpin family E member 1
SERPING1	710	SERPING1	serpin family G member 1
SH2B2	10603	SH2B2	SH2B adaptor protein 2
SIRT2	22933	SIRT2	sirtuin 2
SPARC	6678	SPARC	secreted protein acidic and cysteine rich
TF	7018	TF	transferrin
TFPI2	7980	TFPI2	tissue factor pathway inhibitor 2
THBD	7056	THBD	thrombomodulin
THBS1	7057	THBS1	thrombospondin 1

TIMP1	7076	TIMP1	TIMP metallopeptidase inhibitor 1
TIMP3	7078	TIMP3	TIMP metallopeptidase inhibitor 3 [Sourc...
TMPRSS6	164656	TMPRSS6	transmembrane serine protease 6 [Source:...
USP11	8237	USP11	ubiquitin specific peptidase 11 [Source:...
VWF	7450	VWF	von Willebrand factor [Source:HGNC Symbo...
WDR1	9948	WDR1	WD repeat domain 1 [Source:HGNC Symbol;A...

Table S3 – Coagulation Hallmark in GBM single cell RNAseq dataset

PROBE	*DESCRIPTION (from dataset)*	*RANK IN GENE LIST*	*RANK METRIC SCORE*	*RUNNING ES*	*CORE ENRICHMENT*
SERPING1	serpin family G member 1 [Source:HGNC Symbol;Acc:HGNC:1228]	4	1.858757257	0.03440464	Yes
C1R	complement C1r [Source:HGNC Symbol;Acc:HGNC:1246]	7	1.731820941	0.06656306	Yes
TIMP3	TIMP metallopeptidase inhibitor 3 [Source:HGNC Symbol;Acc:HGNC:11822]	24	1.482592702	0.09323874	Yes
RGN	regucalcin [Source:HGNC Symbol;Acc:HGNC:9989]	51	1.327007532	0.11641632	Yes
CFH	complement factor H [Source:HGNC Symbol;Acc:HGNC:4883]	66	1.272586584	0.13929752	Yes
F3	coagulation factor III, tissue factor [Source:HGNC Symbol;Acc:HGNC:3541]	67	1.267872691	0.16292842	Yes
MMP7	matrix metallopeptidase 7 [Source:HGNC Symbol;Acc:HGNC:7174]	88	1.224679351	0.18455774	Yes
PROS1	protein S [Source:HGNC Symbol;Acc:HGNC:9456]	93	1.209008217	0.20685221	Yes
CTSK	cathepsin K [Source:HGNC Symbol;Acc:HGNC:2536]	115	1.164898157	0.2273075	Yes
C3	complement C3 [Source:HGNC Symbol;Acc:HGNC:1318]	127	1.151113391	0.24810411	Yes
CPQ	carboxypeptidase Q [Source:HGNC Symbol;Acc:HGNC:16910]	140	1.124162197	0.2683386	Yes
CFB	complement factor B [Source:HGNC Symbol;Acc:HGNC:1037]	145	1.121198773	0.28899646	Yes
C1S	complement C1s [Source:HGNC Symbol;Acc:HGNC:1247]	164	1.095129609	0.30833083	Yes
CTSB	cathepsin B [Source:HGNC Symbol;Acc:HGNC:2527]	172	1.089091063	0.3282108	Yes
FN1	fibronectin 1 [Source:HGNC Symbol;Acc:HGNC:3778]	204	1.044075847	0.3458159	Yes
CLU	clusterin [Source:HGNC Symbol;Acc:HGNC:2095]	211	1.036480546	0.3647751	Yes
MMP14	matrix metallopeptidase 14 [Source:HGNC Symbol;Acc:HGNC:7160]	257	0.9872756	0.38048398	Yes
MMP9	matrix metallopeptidase 9 [Source:HGNC Symbol;Acc:HGNC:7176]	398	0.887420774	0.3886482	Yes
THBS1	thrombospondin 1 [Source:HGNC Symbol;Acc:HGNC:11785]	404	0.884098947	0.40482712	Yes
APOA1	apolipoprotein A1 [Source:HGNC Symbol;Acc:HGNC:600]	701	0.767238975	0.40141845	Yes

CSRP1	cysteine and glycine rich protein 1 [Source:HGNC Symbol;Acc:HGNC:2469]	787	0.74096334	0.41014344	Yes
ADAM9	ADAM metallopeptidase domain 9 [Source:HGNC Symbol;Acc:HGNC:216]	922	0.709156394	0.41534412	Yes
LAMP2	lysosomal associated membrane protein 2 [Source:HGNC Symbol;Acc:HGNC:6501]	936	0.707423151	0.42775148	Yes
TF	transferrin [Source:HGNC Symbol;Acc:HGNC:11740]	948	0.705026329	0.44023383	Yes
P2RY1	purinergic receptor P2Y1 [Source:HGNC Symbol;Acc:HGNC:8539]	978	0.699825943	0.45154238	Yes
DPP4	dipeptidyl peptidase 4 [Source:HGNC Symbol;Acc:HGNC:3009]	998	0.696932018	0.46339527	Yes
ANG	angiogenin [Source:HGNC Symbol;Acc:HGNC:483]	1014	0.69333452	0.4754204	Yes
PRSS23	serine protease 23 [Source:HGNC Symbol;Acc:HGNC:14370]	1216	0.652990937	0.47556585	Yes
SERPINE1	serpin family E member 1 [Source:HGNC Symbol;Acc:HGNC:8583]	1336	0.630359411	0.48019528	Yes
HTRA1	HtrA serine peptidase 1 [Source:HGNC Symbol;Acc:HGNC:9476]	1356	0.627792537	0.49075952	Yes
C2	complement C2 [Source:HGNC Symbol;Acc:HGNC:1248]	1434	0.615044415	0.49761623	Yes
C1QA	complement C1q A chain [Source:HGNC Symbol;Acc:HGNC:1241]	1468	0.610916138	0.50702834	Yes
CAPN2	calpain 2 [Source:HGNC Symbol;Acc:HGNC:1479]	1534	0.600276709	0.5143277	Yes
CTSH	cathepsin H [Source:HGNC Symbol;Acc:HGNC:2535]	1768	0.572178602	0.51105255	Yes
HPN	hepsin [Source:HGNC Symbol;Acc:HGNC:5155]	1779	0.571293354	0.5211022	Yes
ACOX2	acyl-CoA oxidase 2 [Source:HGNC Symbol;Acc:HGNC:120]	1801	0.567798734	0.5304286	Yes
F8	coagulation factor VIII [Source:HGNC Symbol;Acc:HGNC:3546]	2010	0.542892575	0.52810323	Yes
CTSO	cathepsin O [Source:HGNC Symbol;Acc:HGNC:2542]	2019	0.541721463	0.53772134	Yes
SIRT2	sirtuin 2 [Source:HGNC Symbol;Acc:HGNC:10886]	2238	0.519492567	0.5343616	Yes
MMP1	matrix metallopeptidase 1 [Source:HGNC Symbol;Acc:HGNC:7155]	2242	0.519201934	0.5438591	Yes

SERPINB2	serpin family B member 2 [Source:HGNC Symbol;Acc:HGNC:8584]	2339	0.509779871	0.54761714	Yes
GNG12	G protein subunit gamma 12 [Source:HGNC Symbol;Acc:HGNC:19663]	2362	0.507722497	0.555764	Yes
TIMP1	TIMP metallopeptidase inhibitor 1 [Source:HGNC Symbol;Acc:HGNC:11820]	2380	0.506691396	0.5641908	Yes
A2M	alpha-2-macroglobulin [Source:HGNC Symbol;Acc:HGNC:7]	2606	0.485911191	0.5597864	No
RABIF	RAB interacting factor [Source:HGNC Symbol;Acc:HGNC:9797]	2970	0.45365566	0.5465247	No
PLAU	plasminogen activator, urokinase [Source:HGNC Symbol;Acc:HGNC:9052]	3014	0.449748307	0.55233467	No
MSRB2	methionine sulfoxide reductase B2 [Source:HGNC Symbol;Acc:HGNC:17061]	3406	0.422940761	0.53682536	No
MMP10	matrix metallopeptidase 10 [Source:HGNC Symbol;Acc:HGNC:7156]	3564	0.411859334	0.5351089	No
MMP3	matrix metallopeptidase 3 [Source:HGNC Symbol;Acc:HGNC:7173]	3596	0.409843028	0.5408931	No
PEF1	penta-EF-hand domain containing 1 [Source:HGNC Symbol;Acc:HGNC:30009]	3752	0.400109619	0.5390773	No
BMP1	bone morphogenetic protein 1 [Source:HGNC Symbol;Acc:HGNC:1067]	3973	0.38545236	0.5330996	No
C8A	complement C8 alpha chain [Source:HGNC Symbol;Acc:HGNC:1352]	4090	0.378324747	0.53321105	No
ITGA2	integrin subunit alpha 2 [Source:HGNC Symbol;Acc:HGNC:6137]	4320	0.363684267	0.52628917	No
FYN	FYN proto-oncogene, Src family tyrosine kinase [Source:HGNC Symbol;Acc:HGNC:4037]	5112	0.315252423	0.48484218	No
KLF7	Kruppel like factor 7 [Source:HGNC Symbol;Acc:HGNC:6350]	5273	0.306273729	0.48097834	No
SPARC	secreted protein acidic and cysteine rich [Source:HGNC Symbol;Acc:HGNC:11219]	5290	0.305469126	0.48571452	No
GSN	gelsolin [Source:HGNC Symbol;Acc:HGNC:4620]	5498	0.293553323	0.47880176	No
F2RL2	coagulation factor II thrombin receptor like 2 [Source:HGNC Symbol;Acc:HGNC:3539]	5505	0.293119878	0.48390603	No
F12	coagulation factor XII [Source:HGNC Symbol;Acc:HGNC:3530]	5536	0.291603953	0.4875462	No

F10	coagulation factor X [Source:HGNC Symbol;Acc:HGNC:3528]	5734	0.278484762	0.48095086	No
ANXA1	annexin A1 [Source:HGNC Symbol;Acc:HGNC:533]	5743	0.278169185	0.48565683	No
ITIH1	inter-alpha-trypsin inhibitor heavy chain 1 [Source:HGNC Symbol;Acc:HGNC:6166]	5792	0.275621474	0.48792225	No
RAC1	Rac family small GTPase 1 [Source:HGNC Symbol;Acc:HGNC:9801]	5978	0.265949965	0.48181117	No
LGMN	legumain [Source:HGNC Symbol;Acc:HGNC:9472]	5981	0.265852273	0.48664653	No
F2	coagulation factor II, thrombin [Source:HGNC Symbol;Acc:HGNC:3535]	6127	0.257644385	0.48277372	No
CTSE	cathepsin E [Source:HGNC Symbol;Acc:HGNC:2530]	6165	0.255779058	0.48532742	No
APOC1	apolipoprotein C1 [Source:HGNC Symbol;Acc:HGNC:607]	6289	0.248811319	0.48260617	No
S100A1	S100 calcium binding protein A1 [Source:HGNC Symbol;Acc:HGNC:10486]	6558	0.235948414	0.47097033	No
CASP9	caspase 9 [Source:HGNC Symbol;Acc:HGNC:1511]	6645	0.231642634	0.47014266	No
GP1BA	glycoprotein Ib platelet subunit alpha [Source:HGNC Symbol;Acc:HGNC:4439]	6701	0.228389263	0.47110897	No
ITGB3	integrin subunit beta 3 [Source:HGNC Symbol;Acc:HGNC:6156]	6706	0.228202447	0.47512296	No
CFD	complement factor D [Source:HGNC Symbol;Acc:HGNC:2771]	6847	0.220830202	0.47086313	No
SH2B2	SH2B adaptor protein 2 [Source:HGNC Symbol;Acc:HGNC:17381]	6895	0.217357054	0.47210243	No
MST1	macrophage stimulating 1 [Source:HGNC Symbol;Acc:HGNC:7380]	7182	0.204532117	0.45880416	No
KLKB1	kallikrein B1 [Source:HGNC Symbol;Acc:HGNC:6371]	7484	0.189153284	0.44432187	No
RAPGEF3	Rap guanine nucleotide exchange factor 3 [Source:HGNC Symbol;Acc:HGNC:16629]	7606	0.183105484	0.4404956	No
FBN1	fibrillin 1 [Source:NCBI gene;Acc:2200]	8051	0.160497248	0.41692403	No
DCT	dopachrome tautomerase [Source:HGNC Symbol;Acc:HGNC:2709]	8264	0.15137431	0.40706217	No
PDGFB	platelet derived growth factor subunit B [Source:HGNC Symbol;Acc:HGNC:8800]	8291	0.150394112	0.40830976	No

GNB2	G protein subunit beta 2 [Source:HGNC Symbol;Acc:HGNC:4398]	8378	0.146109596	0.4058879	No
CAPN5	calpain 5 [Source:HGNC Symbol;Acc:HGNC:1482]	8430	0.143585399	0.40551293	No
FGA	fibrinogen alpha chain [Source:HGNC Symbol;Acc:HGNC:3661]	8564	0.137032658	0.40011007	No
PROZ	protein Z, vitamin K dependent plasma glycoprotein [Source:HGNC Symbol;Acc:HGNC:9460]	8747	0.128526777	0.39161715	No
TMPRSS6	transmembrane serine protease 6 [Source:HGNC Symbol;Acc:HGNC:16517]	8955	0.118119344	0.3814346	No
KLK8	kallikrein related peptidase 8 [Source:HGNC Symbol;Acc:HGNC:6369]	9310	0.104283385	0.36219966	No
MMP11	matrix metallopeptidase 11 [Source:HGNC Symbol;Acc:HGNC:7157]	9434	0.102211468	0.35674605	No
PREP	prolyl endopeptidase [Source:HGNC Symbol;Acc:HGNC:9358]	9544	0.09728954	0.35203826	No
C8G	complement C8 gamma chain [Source:HGNC Symbol;Acc:HGNC:1354]	9679	0.089967869	0.34569836	No
F11	coagulation factor XI [Source:HGNC Symbol;Acc:HGNC:3529]	9725	0.087599374	0.34463885	No
FURIN	furin, paired basic amino acid cleaving enzyme [Source:HGNC Symbol;Acc:HGNC:8568]	9859	0.080926701	0.33819026	No
LTA4H	leukotriene A4 hydrolase [Source:HGNC Symbol;Acc:HGNC:6710]	10318	0.057398278	0.31185952	No
LRP1	LDL receptor related protein 1 [Source:HGNC Symbol;Acc:HGNC:6692]	10461	0.049431548	0.30428547	No
CD9	CD9 molecule [Source:HGNC Symbol;Acc:HGNC:1709]	10787	0.031133741	0.28542215	No
MBL2	mannose binding lectin 2 [Source:HGNC Symbol;Acc:HGNC:6922]	10798	0.030490754	0.28539217	No
PF4	platelet factor 4 [Source:HGNC Symbol;Acc:HGNC:8861]	10938	0.023180235	0.27750832	No
PLEK	pleckstrin [Source:HGNC Symbol;Acc:HGNC:9070]	11296	0.002992843	0.25620604	No
APOC3	apolipoprotein C3 [Source:HGNC Symbol;Acc:HGNC:610]	11395	0	0.25034305	No
GP9	glycoprotein IX platelet [Source:HGNC Symbol;Acc:HGNC:4444]	11526	0	0.2425656	No

HNF4A	hepatocyte nuclear factor 4 alpha [Source:HGNC Symbol;Acc:HGNC:5024]	11590	0	0.23879653	No
PROC	protein C, inactivator of coagulation factors Va and VIIIa [Source:HGNC Symbol;Acc:HGNC:9451]	11598	0	0.23837775	No
GDA	guanine deaminase [Source:HGNC Symbol;Acc:HGNC:4212]	12564	-0.003939512	0.1807186	No
CPB2	carboxypeptidase B2 [Source:HGNC Symbol;Acc:HGNC:2300]	12760	-0.015130591	0.16933444	No
ARF4	ADP ribosylation factor 4 [Source:HGNC Symbol;Acc:HGNC:655]	12860	-0.020632811	0.16379617	No
SERPINC1	serpin family C member 1 [Source:HGNC Symbol;Acc:HGNC:775]	12920	-0.025174599	0.16073562	No
ISCU	iron-sulfur cluster assembly enzyme [Source:HGNC Symbol;Acc:HGNC:29882]	13210	-0.042045232	0.14422941	No
PLG	plasminogen [Source:HGNC Symbol;Acc:HGNC:9071]	13386	-0.053980973	0.13476588	No
CRIP2	cysteine rich protein 2 [Source:HGNC Symbol;Acc:HGNC:2361]	13492	-0.061113626	0.12962314	No
MMP8	matrix metallopeptidase 8 [Source:HGNC Symbol;Acc:HGNC:7175]	13567	-0.06680312	0.12644108	No
FGG	fibrinogen gamma chain [Source:HGNC Symbol;Acc:HGNC:3694]	13807	-0.083236799	0.11369393	No
F9	coagulation factor IX [Source:HGNC Symbol;Acc:HGNC:3551]	13830	-0.084891073	0.11395997	No
HMGCS2	3-hydroxy-3-methylglutaryl-CoA synthase 2 [Source:HGNC Symbol;Acc:HGNC:5008]	13853	-0.086663701	0.11425904	No
CPN1	carboxypeptidase N subunit 1 [Source:HGNC Symbol;Acc:HGNC:2312]	13905	-0.091019072	0.112904325	No
TFPI2	tissue factor pathway inhibitor 2 [Source:HGNC Symbol;Acc:HGNC:11761]	13977	-0.09581954	0.11044255	No
VWF	von Willebrand factor [Source:HGNC Symbol;Acc:HGNC:12726]	14074	-0.102724299	0.10661381	No
OLR1	oxidized low density lipoprotein receptor 1 [Source:HGNC Symbol;Acc:HGNC:8133]	14472	-0.121970005	0.08513599	No
MMP2	matrix metallopeptidase 2 [Source:HGNC Symbol;Acc:HGNC:7166]	14486	-0.123156697	0.086653665	No
F13B	coagulation factor XIII B chain [Source:HGNC Symbol;Acc:HGNC:3534]	14559	-0.128719732	0.084745266	No

PLAT	plasminogen activator, tissue type [Source:HGNC Symbol;Acc:HGNC:9051]	14714	-0.143058568	0.07819834	No
C9	complement C9 [Source:HGNC Symbol;Acc:HGNC:1358]	14816	-0.153489873	0.07501665	No
THBD	thrombomodulin [Source:HGNC Symbol;Acc:HGNC:11784]	15220	-0.191700235	0.054479517	No
MASP2	mannan binding lectin serine peptidase 2 [Source:HGNC Symbol;Acc:HGNC:6902]	15643	-0.254454553	0.033975314	No
CTSV	cathepsin V [Source:HGNC Symbol;Acc:HGNC:2538]	15844	-0.287521034	0.027368898	No
HRG	histidine rich glycoprotein [Source:HGNC Symbol;Acc:HGNC:5181]	15854	-0.289986432	0.032235295	No
MEP1A	meprin A subunit alpha [Source:HGNC Symbol;Acc:HGNC:7015]	16001	-0.319728732	0.0294598	No
MMP15	matrix metallopeptidase 15 [Source:HGNC Symbol;Acc:HGNC:7161]	16184	-0.365612179	0.025385741	No
COMP	cartilage oligomeric matrix protein [Source:HGNC Symbol;Acc:HGNC:2227]	16187	-0.365708798	0.032082252	No
LEFTY2	left-right determination factor 2 [Source:HGNC Symbol;Acc:HGNC:3122]	16220	-0.374752462	0.037152525	No

Table S4 – Coagulation Hallmark in GBM TCGA dataset

PROBE	*DESCRIPTION (from dataset)*	*RANK IN GENE LIST*	*RANK METRIC SCORE*	*RUNNING ES*	*CORE ENRICHMENT*
F3	coagulation factor III, tissue factor [Source:HGNC Symbol;Acc:HGNC:3541]	36	0.910183012	0.0216108	Yes
ADAM9	ADAM metallopeptidase domain 9 [Source:HGNC Symbol;Acc:HGNC:216]	74	0.837914586	0.04129853	Yes
C1R	complement C1r [Source:HGNC Symbol;Acc:HGNC:1246]	117	0.788890839	0.05944972	Yes
ANG	angiogenin [Source:HGNC Symbol;Acc:HGNC:483]	179	0.745010436	0.07544571	Yes
ANXA1	annexin A1 [Source:HGNC Symbol;Acc:HGNC:533]	180	0.743535757	0.09467874	Yes
CFI	complement factor I [Source:HGNC Symbol;Acc:HGNC:5394]	205	0.728622615	0.1122374	Yes
PROS1	protein S [Source:HGNC Symbol;Acc:HGNC:9456]	209	0.72649169	0.13086846	Yes
SERPING1	serpin family G member 1 [Source:HGNC Symbol;Acc:HGNC:1228]	356	0.668031633	0.1403095	Yes
PLAU	plasminogen activator, urokinase [Source:HGNC Symbol;Acc:HGNC:9052]	359	0.667090178	0.15745772	Yes
C1S	complement C1s [Source:HGNC Symbol;Acc:HGNC:1247]	365	0.665393651	0.17440099	Yes
MAFF	MAF bZIP transcription factor F [Source:HGNC Symbol;Acc:HGNC:6780]	478	0.627346873	0.18461514	Yes
GNG12	G protein subunit gamma 12 [Source:HGNC Symbol;Acc:HGNC:19663]	536	0.609083951	0.19730988	Yes
CPQ	carboxypeptidase Q [Source:HGNC Symbol;Acc:HGNC:16910]	612	0.593698263	0.20864022	Yes

CFB	complement factor B [Source:HGNC Symbol;Acc:HGNC:1037]	634	0.590267777	0.22278114	Yes
FURIN	furin, paired basic amino acid cleaving enzyme [Source:HGNC Symbol;Acc:HGNC:8568]	647	0.587606013	0.23733643	Yes
SERPINE1	serpin family E member 1 [Source:HGNC Symbol;Acc:HGNC:8583]	657	0.584779799	0.2519797	Yes
WDR1	WD repeat domain 1 [Source:HGNC Symbol;Acc:HGNC:12754]	725	0.57375741	0.26322374	Yes
CLU	clusterin [Source:HGNC Symbol;Acc:HGNC:2095]	770	0.565582335	0.27549124	Yes
THBD	thrombomodulin [Source:HGNC Symbol;Acc:HGNC:11784]	777	0.564702988	0.28977624	Yes
S100A13	S100 calcium binding protein A13 [Source:HGNC Symbol;Acc:HGNC:10490]	803	0.561137557	0.3029489	Yes
TIMP1	TIMP metallopeptidase inhibitor 1 [Source:HGNC Symbol;Acc:HGNC:11820]	845	0.555727422	0.31512254	Yes
CTSB	cathepsin B [Source:HGNC Symbol;Acc:HGNC:2527]	952	0.539616168	0.3233895	Yes
SPARC	secreted protein acidic and cysteine rich [Source:HGNC Symbol;Acc:HGNC:11219]	1050	0.526174605	0.331792	Yes
THBS1	thrombospondin 1 [Source:HGNC Symbol;Acc:HGNC:11785]	1080	0.523187995	0.34376824	Yes
ITGB3	integrin subunit beta 3 [Source:HGNC Symbol;Acc:HGNC:6156]	1112	0.519691527	0.35554665	Yes
SERPINA1	serpin family A member 1 [Source:HGNC Symbol;Acc:HGNC:8941]	1149	0.514729917	0.36692828	Yes
CAPN2	calpain 2 [Source:HGNC Symbol;Acc:HGNC:1479]	1187	0.511399209	0.37817004	Yes
ACOX2	acyl-CoA oxidase 2 [Source:HGNC Symbol;Acc:HGNC:120]	1248	0.505106151	0.38801414	Yes

ITGA2	integrin subunit alpha 2 [Source:HGNC Symbol;Acc:HGNC:6137]	1315	0.498697251	0.3973703	Yes
C3	complement C3 [Source:HGNC Symbol;Acc:HGNC:1318]	1322	0.497975647	0.40992928	Yes
LTA4H	leukotriene A4 hydrolase [Source:HGNC Symbol;Acc:HGNC:6710]	1344	0.495357901	0.42161515	Yes
RAC1	Rac family small GTPase 1 [Source:HGNC Symbol;Acc:HGNC:9801]	1454	0.486291409	0.4283417	Yes
PRSS23	serine protease 23 [Source:HGNC Symbol;Acc:HGNC:14370]	1649	0.467956156	0.4300302	Yes
LAMP2	lysosomal associated membrane protein 2 [Source:HGNC Symbol;Acc:HGNC:6501]	1663	0.466986984	0.44141176	Yes
HTRA1	HtrA serine peptidase 1 [Source:HGNC Symbol;Acc:HGNC:9476]	1743	0.459745437	0.44906238	Yes
P2RY1	purinergic receptor P2Y1 [Source:HGNC Symbol;Acc:HGNC:8539]	1836	0.452348351	0.45582366	Yes
PECAM1	platelet and endothelial cell adhesion molecule 1 [Source:HGNC Symbol;Acc:HGNC:8823]	1911	0.447104067	0.4634157	Yes
DPP4	dipeptidyl peptidase 4 [Source:HGNC Symbol;Acc:HGNC:3009]	2061	0.435605168	0.4666835	Yes
CD9	CD9 molecule [Source:HGNC Symbol;Acc:HGNC:1709]	2232	0.42399025	0.46852335	Yes
LRP1	LDL receptor related protein 1 [Source:HGNC Symbol;Acc:HGNC:6692]	2306	0.419745207	0.47546142	Yes
CTSO	cathepsin O [Source:HGNC Symbol;Acc:HGNC:2542]	2333	0.418025851	0.4848785	Yes
CSRP1	cysteine and glycine rich protein 1 [Source:HGNC Symbol;Acc:HGNC:2469]	2719	0.393649101	0.47438988	No

C1QA	complement C1q A chain [Source:HGNC Symbol;Acc:HGNC:1241]	2885	0.383368939	0.47544742	No
A2M	alpha-2-macroglobulin [Source:HGNC Symbol;Acc:HGNC:7]	3179	0.368489683	0.46924758	No
DUSP6	dual specificity phosphatase 6 [Source:HGNC Symbol;Acc:HGNC:3072]	3322	0.3599374	0.4709339	No
ARF4	ADP ribosylation factor 4 [Source:HGNC Symbol;Acc:HGNC:655]	3341	0.358831972	0.47924936	No
RGN	regucalcin [Source:HGNC Symbol;Acc:HGNC:9989]	3764	0.338168919	0.46533906	No
GNB2	G protein subunit beta 2 [Source:HGNC Symbol;Acc:HGNC:4398]	3958	0.329586983	0.46350205	No
PLEK	pleckstrin [Source:HGNC Symbol;Acc:HGNC:9070]	4420	0.30941993	0.44675413	No
PEF1	penta-EF-hand domain containing 1 [Source:HGNC Symbol;Acc:HGNC:30009]	4647	0.299046636	0.44235533	No
KLF7	Kruppel like factor 7 [Source:HGNC Symbol;Acc:HGNC:6350]	4799	0.292868614	0.44182357	No
APOC1	apolipoprotein C1 [Source:HGNC Symbol;Acc:HGNC:607]	4915	0.287545413	0.443087	No
C2	complement C2 [Source:HGNC Symbol;Acc:HGNC:1248]	5177	0.277578861	0.43625373	No
APOC2	apolipoprotein C2 [Source:HGNC Symbol;Acc:HGNC:609]	5365	0.271299571	0.43323115	No
TFPI2	tissue factor pathway inhibitor 2 [Source:HGNC Symbol;Acc:HGNC:11761]	5775	0.255332977	0.4178761	No
PDGFB	platelet derived growth factor subunit B [Source:HGNC Symbol;Acc:HGNC:8800]	6230	0.239396691	0.39969274	No
DUSP14	dual specificity phosphatase 14 [Source:HGNC Symbol;Acc:HGNC:17007]	6344	0.235702962	0.39972255	No

CRIP2	cysteine rich protein 2 [Source:HGNC Symbol;Acc:HGNC:2361]	6400	0.233463585	0.40280852	No
SERPINC1	serpin family C member 1 [Source:HGNC Symbol;Acc:HGNC:775]	6457	0.23143366	0.4057883	No
VWF	von Willebrand factor [Source:HGNC Symbol;Acc:HGNC:12726]	6464	0.231177896	0.41144603	No
APOA1	apolipoprotein A1 [Source:HGNC Symbol;Acc:HGNC:600]	6561	0.227548048	0.41217765	No
ITIH1	inter-alpha-trypsin inhibitor heavy chain 1 [Source:HGNC Symbol;Acc:HGNC:6166]	6587	0.22667031	0.41669863	No
LGMN	legumain [Source:HGNC Symbol;Acc:HGNC:9472]	6672	0.224245638	0.41798913	No
MMP14	matrix metallopeptidase 14 [Source:HGNC Symbol;Acc:HGNC:7160]	7139	0.207995534	0.3983492	No
OLR1	oxidized low density lipoprotein receptor 1 [Source:HGNC Symbol;Acc:HGNC:8133]	7249	0.204761878	0.3977934	No
MMP3	matrix metallopeptidase 3 [Source:HGNC Symbol;Acc:HGNC:7173]	7396	0.19982864	0.39512345	No
FN1	fibronectin 1 [Source:HGNC Symbol;Acc:HGNC:3778]	7698	0.189764217	0.38387102	No
CFD	complement factor D [Source:HGNC Symbol;Acc:HGNC:2771]	7734	0.188399687	0.38686514	No
LEFTY2	left-right determination factor 2 [Source:HGNC Symbol;Acc:HGNC:3122]	7743	0.188082263	0.39130074	No
PLAT	plasminogen activator, tissue type [Source:HGNC Symbol;Acc:HGNC:9051]	7845	0.183996364	0.39063734	No
ISCU	iron-sulfur cluster assembly enzyme [Source:HGNC Symbol;Acc:HGNC:29882]	7925	0.180842265	0.39107358	No

F12	coagulation factor XII [Source:HGNC Symbol;Acc:HGNC:3530]	8022	0.177817017	0.3905188	No
MMP8	matrix metallopeptidase 8 [Source:HGNC Symbol;Acc:HGNC:7175]	8129	0.173071966	0.38930437	No
PF4	platelet factor 4 [Source:HGNC Symbol;Acc:HGNC:8861]	8842	0.150620878	0.3549723	No
TIMP3	TIMP metallopeptidase inhibitor 3 [Source:HGNC Symbol;Acc:HGNC:11822]	8905	0.148370564	0.35548133	No
F8	coagulation factor VIII [Source:HGNC Symbol;Acc:HGNC:3546]	9168	0.139366686	0.34501922	No
GSN	gelsolin [Source:HGNC Symbol;Acc:HGNC:4620]	9362	0.132928893	0.33809528	No
SERPINB2	serpin family B member 2 [Source:HGNC Symbol;Acc:HGNC:8584]	9744	0.119747974	0.3207364	No
CTSH	cathepsin H [Source:HGNC Symbol;Acc:HGNC:2535]	9792	0.118884861	0.3212881	No
TMPRSS6	transmembrane serine protease 6 [Source:HGNC Symbol;Acc:HGNC:16517]	9905	0.115040839	0.31825045	No
MMP7	matrix metallopeptidase 7 [Source:HGNC Symbol;Acc:HGNC:7174]	9947	0.113511942	0.3189853	No
COMP	cartilage oligomeric matrix protein [Source:HGNC Symbol;Acc:HGNC:2227]	9989	0.111757852	0.31967482	No
MMP9	matrix metallopeptidase 9 [Source:HGNC Symbol;Acc:HGNC:7176]	10278	0.101687148	0.30684206	No
PREP	prolyl endopeptidase [Source:HGNC Symbol;Acc:HGNC:9358]	10704	0.086265527	0.2862547	No
HRG	histidine rich glycoprotein [Source:HGNC Symbol;Acc:HGNC:5181]	10785	0.084256619	0.28413886	No

FYN	FYN proto-oncogene, Src family tyrosine kinase [Source:HGNC Symbol;Acc:HGNC:4037]	10920	0.079102337	0.27899036	No
BMP1	bone morphogenetic protein 1 [Source:HGNC Symbol;Acc:HGNC:1067]	11111	0.071977854	0.27065086	No
APOC3	apolipoprotein C3 [Source:HGNC Symbol;Acc:HGNC:610]	11267	0.066845916	0.26405782	No
CTSK	cathepsin K [Source:HGNC Symbol;Acc:HGNC:2536]	11327	0.065168977	0.26257578	No
MMP1	matrix metallopeptidase 1 [Source:HGNC Symbol;Acc:HGNC:7155]	11802	0.047368143	0.23835137	No
GDA	guanine deaminase [Source:HGNC Symbol;Acc:HGNC:4212]	11989	0.040571615	0.22941425	No
MASP2	mannan binding lectin serine peptidase 2 [Source:HGNC Symbol;Acc:HGNC:6902]	12253	0.02956792	0.21605828	No
PROC	protein C, inactivator of coagulation factors Va and VIIIa [Source:HGNC Symbol;Acc:HGNC:9451]	12277	0.028340485	0.21555647	No
MMP10	matrix metallopeptidase 10 [Source:HGNC Symbol;Acc:HGNC:7156]	12574	0.015488714	0.2000645	No
FGG	fibrinogen gamma chain [Source:HGNC Symbol;Acc:HGNC:3694]	12606	0.014458778	0.19877407	No
C8G	complement C8 gamma chain [Source:HGNC Symbol;Acc:HGNC:1354]	12784	0.005403371	0.1894105	No
GP1BA	glycoprotein Ib platelet subunit alpha [Source:HGNC Symbol;Acc:HGNC:4439]	12831	0.003406005	0.1870288	No
F2	coagulation factor II, thrombin [Source:HGNC Symbol;Acc:HGNC:3535]	13093	-1.16E-09	0.17301537	No
CFH	complement factor H [Source:HGNC Symbol;Acc:HGNC:4883]	13200	-0.004291414	0.16743511	No

MST1	macrophage stimulating 1 [Source:HGNC Symbol;Acc:HGNC:7380]	13210	-0.004780144	0.16707553	No
GP9	glycoprotein IX platelet [Source:HGNC Symbol;Acc:HGNC:4444]	13238	-0.006370975	0.16579066	No
RABIF	RAB interacting factor [Source:HGNC Symbol;Acc:HGNC:9797]	13293	-0.009427322	0.16313519	No
MMP11	matrix metallopeptidase 11 [Source:HGNC Symbol;Acc:HGNC:7157]	13456	-0.017222032	0.15488268	No
KLKB1	kallikrein B1 [Source:HGNC Symbol;Acc:HGNC:6371]	13518	-0.020154944	0.15212886	No
CAPN5	calpain 5 [Source:HGNC Symbol;Acc:HGNC:1482]	13565	-0.022612603	0.15024398	No
FBN1	fibrillin 1 [Source:NCBI gene;Acc:2200]	13674	-0.027810747	0.14516471	No
USP11	ubiquitin specific peptidase 11 [Source:HGNC Symbol;Acc:HGNC:12609]	13697	-0.029041309	0.14473471	No
CTSE	cathepsin E [Source:HGNC Symbol;Acc:HGNC:2530]	13717	-0.029902011	0.14448805	No
C8B	complement C8 beta chain [Source:HGNC Symbol;Acc:HGNC:1353]	13952	-0.03968934	0.13295093	No
SH2B2	SH2B adaptor protein 2 [Source:HGNC Symbol;Acc:HGNC:17381]	14029	-0.043134294	0.12998615	No
C8A	complement C8 alpha chain [Source:HGNC Symbol;Acc:HGNC:1352]	14239	-0.052315723	0.12011793	No
PLG	plasminogen [Source:HGNC Symbol;Acc:HGNC:9071]	14265	-0.053376053	0.12015632	No
CPB2	carboxypeptidase B2 [Source:HGNC Symbol;Acc:HGNC:2300]	14498	-0.064178921	0.10936006	No
MSRB2	methionine sulfoxide reductase B2 [Source:HGNC Symbol;Acc:HGNC:17061]	14565	-0.066644408	0.10754032	No

MBL2	mannose binding lectin 2 [Source:HGNC Symbol;Acc:HGNC:6922]	14578	-0.066845916	0.10862513	No
CASP9	caspase 9 [Source:HGNC Symbol;Acc:HGNC:1511]	15055	-0.090294726	0.08540373	No
FGA	fibrinogen alpha chain [Source:HGNC Symbol;Acc:HGNC:3661]	15263	-0.099694513	0.07686844	No
MMP2	matrix metallopeptidase 2 [Source:HGNC Symbol;Acc:HGNC:7166]	15806	-0.130969331	0.05115555	No
PROZ	protein Z, vitamin K dependent plasma glycoprotein [Source:HGNC Symbol;Acc:HGNC:9460]	15922	-0.13684313	0.04852077	No
C9	complement C9 [Source:HGNC Symbol;Acc:HGNC:1358]	16135	-0.14724943	0.04094712	No
RAPGEF3	Rap guanine nucleotide exchange factor 3 [Source:HGNC Symbol;Acc:HGNC:16629]	16210	-0.150888562	0.04087699	No
TF	transferrin [Source:HGNC Symbol;Acc:HGNC:11740]	16284	-0.15382506	0.04093652	No
MEP1A	meprin A subunit alpha [Source:HGNC Symbol;Acc:HGNC:7015]	16579	-0.165011287	0.02941963	No
KLK8	kallikrein related peptidase 8 [Source:HGNC Symbol;Acc:HGNC:6369]	16717	-0.172377214	0.0265228	No
S100A1	S100 calcium binding protein A1 [Source:HGNC Symbol;Acc:HGNC:10486]	16719	-0.172401249	0.0309286	No
F11	coagulation factor XI [Source:HGNC Symbol;Acc:HGNC:3529]	16767	-0.174834251	0.03292755	No
F2RL2	coagulation factor II thrombin receptor like 2 [Source:HGNC Symbol;Acc:HGNC:3539]	16886	-0.181637213	0.03129038	No
HNF4A	hepatocyte nuclear factor 4 alpha [Source:HGNC Symbol;Acc:HGNC:5024]	17244	-0.206598282	0.01746667	No

HPN	hepsin [Source:HGNC Symbol;Acc:HGNC:5155]	17261	-0.207463175	0.02197406	No
F13B	coagulation factor XIII B chain [Source:HGNC Symbol;Acc:HGNC:3534]	17376	-0.215106457	0.0214174	No
F9	coagulation factor IX [Source:HGNC Symbol;Acc:HGNC:3551]	17471	-0.223493546	0.02215152	No
CTSV	cathepsin V [Source:HGNC Symbol;Acc:HGNC:2538]	17541	-0.228914499	0.02436815	No
MMP15	matrix metallopeptidase 15 [Source:HGNC Symbol;Acc:HGNC:7161]	17918	-0.265861928	0.01105728	No
F10	coagulation factor X [Source:HGNC Symbol;Acc:HGNC:3528]	18094	-0.288691461	0.00912888	No
DCT	dopachrome tautomerase [Source:HGNC Symbol;Acc:HGNC:2709]	18305	-0.321630776	0.00617332	No
HMGCS2	3-hydroxy-3-methylglutaryl-CoA synthase 2 [Source:HGNC Symbol;Acc:HGNC:5008]	18425	-0.349797219	0.00883226	No
SIRT2	sirtuin 2 [Source:HGNC Symbol;Acc:HGNC:10886]	18442	-0.353902817	0.01712759	No

Gel scans

Dacomitinib (PF) Treatment – Wester Blot Scans

Total EGFR

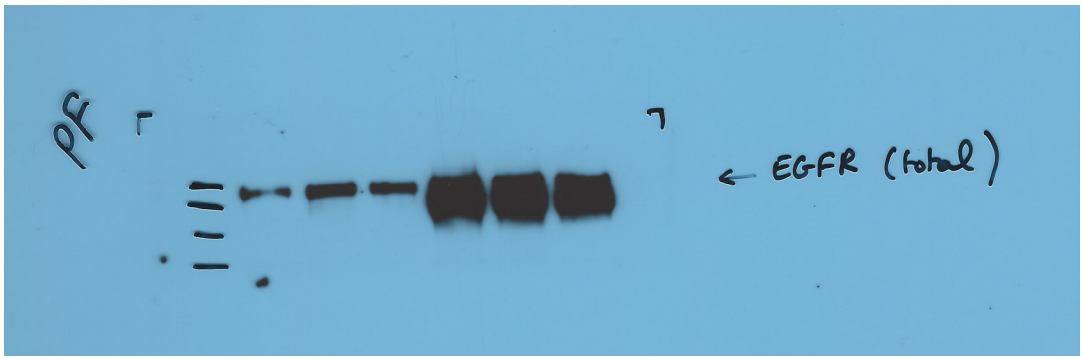

Total EGFR

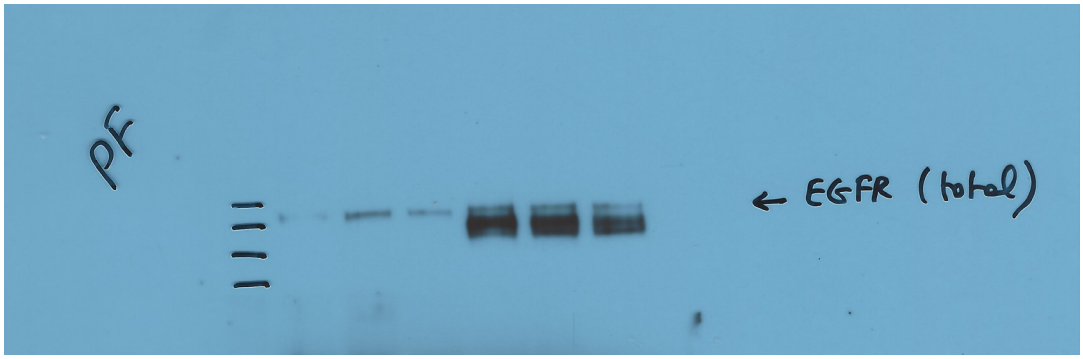

pEGFR

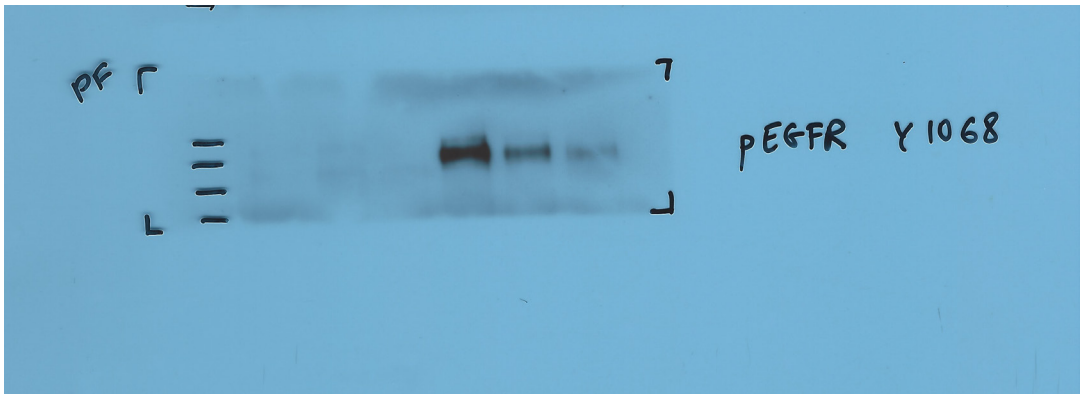

pEGFR

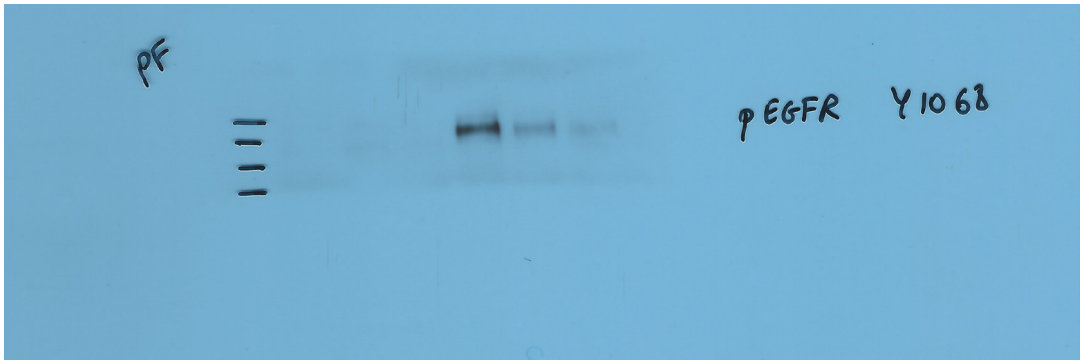

PDPN

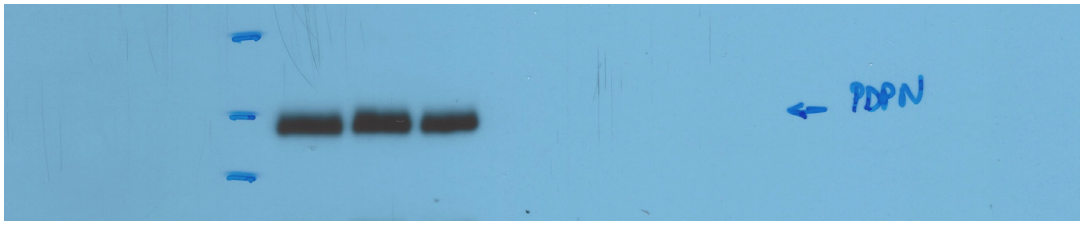

Actin

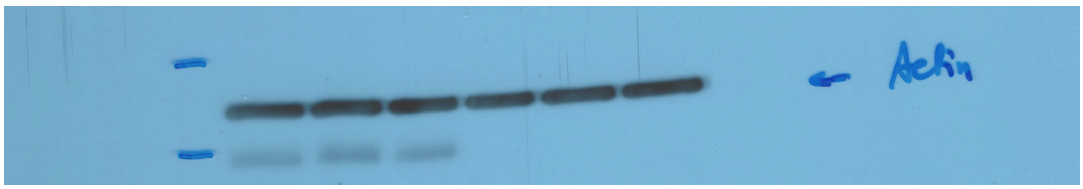

Pictilisib Treatment – Wester Blot Scans

Total AKT

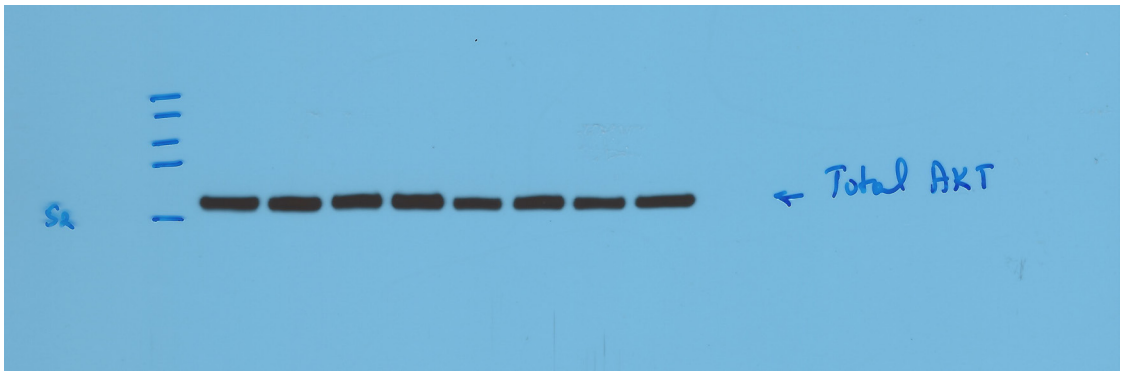

pAKT

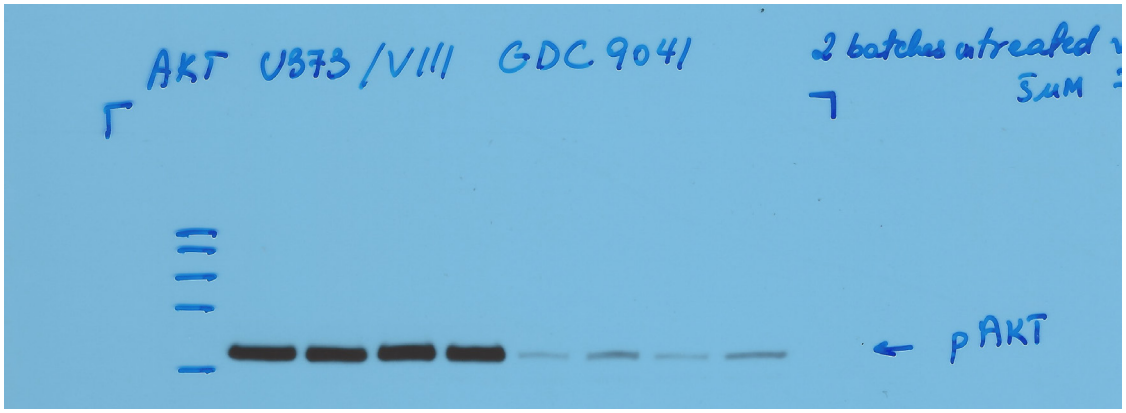

pAKT

PDPN

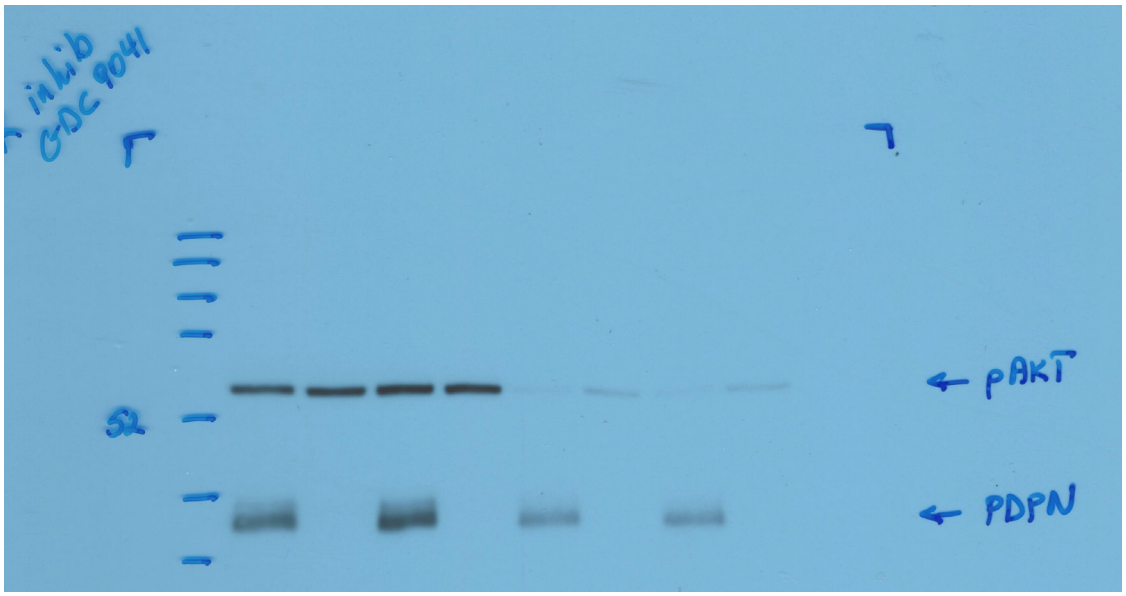

Actin

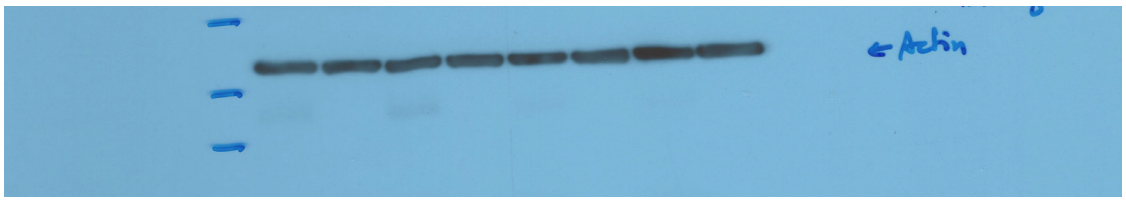

5-Aza Treatment – Wester Blot Scans

PDPN

Actin

UNC1999 Treatment – Wester Blot Scans

PDPN

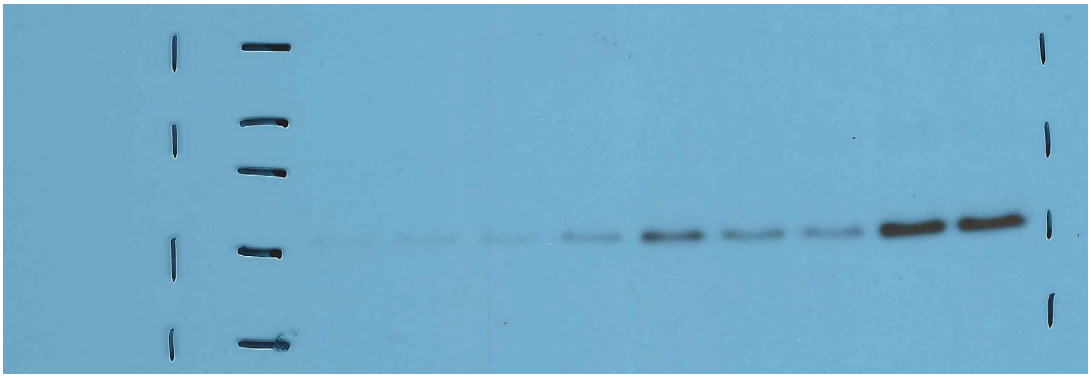

Actin

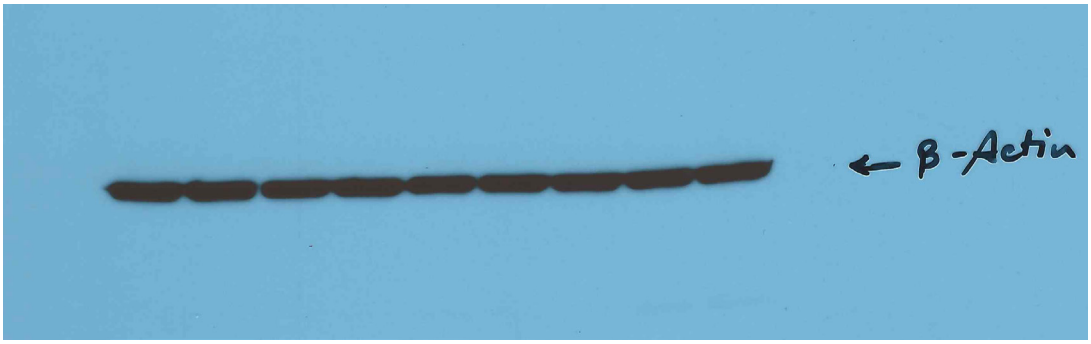

SUPPLEMENTARY METHODS (Tawil et al)

Cell lines, culture conditions, reagents and treatments

Cell culture conditions have been previously described[1,2]. Briefly, U373P- and U87P-derived cells were maintained in Dulbecco's Modified Eagle's minimal essential medium (DMEM), supplemented with 10% Fetal Bovine Serum (Multicell FBS) and 1% Penicillin-Streptomycin (Gibco). GBM patient derived glioma stem cell lines (GSC), GSC157 and GSC1079 were derived and characterized as proneural in the laboratory of Ichiro Nakano[3]. GSC lines were maintained as sphere cultures, unless otherwise indicated, in DMEM-F12 media (GIBCO) supplemented with EGF (GIBCO), FGF (GIBCO), Heparin 0.2% (STEMCELL), B27 serum free supplement (GIBCO), Glutamax (GIBCO) and 1% penicillin-streptomycin (P/S) (GIBCO) [2,4].

We used several isogenic variants derived from either U87P or U373P glioma cell lines (Fig. 2A)[1]. Notably, cells that were only maintained in culture and did not undergo passage in mice were designated as parental (U373P, U87P, see below). The corresponding cell lines transfected with EGFRvIII oncogene were designated as U373vIII and U87vIII, respectively, and were generously supplied by late Dr. Abhijit Guha (University of Toronto). U373P cells were also transfected with TF injected subcutaneously and allowed to form primary tumors (PT) in immunodeficient mice after a long latency period, followed by their re-establishment in culture (Fig. 2a). The respective designation of such cell line used in this study is U373TF-G11-PT [1]. Finally, while U373 are indolent and form dormant lesions in mice on rare occasions we were able to isolate tumors from mice injected with these cells and re-establish them in culture (U373-PT). To produce similar, mouse-derived cell lines expressing EGFRvIII, the U373vIII cell line was injected into mice and tumors isolated, dissociated and cultured (U373vIII-PT).

It should be mentioned that batches of U373P and U373vIII cells used in the present study were previously described by their originators[5], extensively characterized[1] and maintained in the laboratory for over 10 years, while exhibiting a remarkable phenotypic stability and data reproducibility. Using short tandem repeat (STR) assays the U373P cells were subsequently assigned genetic identity common with the commercially available U373MG cell line, which was found to be identical with another commercially available U251MG cells, resulting in recent renaming of these cell lines to reflect their common origin (https://www.phe-culturecollections.org.uk/collections/ecacc.aspx). However, the biological properties observed in the case of our U373P cell line maintained from early passage in our laboratory, including their stable, astrocytic, and indolent phenotype, as well as low TF expression[1,6], were found to be different then those described in the literature for more aggressive U373MG cells available commercially[7]. Therefore, we believe that our cells represent a variant, possibly less altered, of the commercially available U373MG cells and we chose to adopt their unique designation, "U373P" to avoid any possible confusion. For all cell lines their designation as "PT" (e.g. U373PT) indicates that the cells were isolated from the primary tumor initiated by the indicated cells in mice (e.g. U373).

For GSCs their serum induced differentiation protocol involved maintenance in DMEM-F12 media supplemented with 10% FBS, 1% P/S and 1% Glutamax. For Dacomitinib treatment, U373P and U373vIII cells were incubated with the drug (PF 00299804) (Selleckchem) at concentrations of 0.125 μM and 1 μM in DMEM supplemented with 10% FBS growth medium replaced every 24hr and extracts for western blot analysis were collected at 72h. For Pictilisib treatment two batches of U373P and U373vIII cells were treated for 72h with the drug (GDC-0941 Catalog No. S1065) at the concentration of 5 μM in DMEM supplemented with 10% Fetal Bovine Serum and

1% Penicillin-Streptomycin, and treatment medium was replaced every 24hr. For 5-aza-2′-deoxycytidine (DAC) treatment. U373P, U373vIII and U87vIII cells were incubated with 5 μM of the drug (Sigma-Aldrich) 24h after plating in growth medium, and drug-containing medium was replaced every 24h. Western blot analysis was performed on extracts harvested 1, 2 and 3 days after the beginning of DAC treatment. For EZH2 inhibitor treatment, U373vIII cells were incubated with the drug (UNC1999; Selleckchem, Catalog No. S7165) at the concentration of 2.5 μM in complete growth medium for 25 days. Drug-supplemented growth medium was replaced every 48hrs. Extracts were collected on days 0, 5, 10, 15, 20 and 25 for western blotting. In combination treatment with Dacomitinib experiment, UNC1999 was used at concentrations of 1.25 μM or 2.5 μM and treatment duration was 7 days followed by western blotting.

Quantitative Real-time q-PCR

The relative mRNA expression levels of PDPN, miR-520g (along with control GAPDH mRNA and U6, respectively) were quantified using real-time PCR analysis[8]. PDPN mRNA levels assessment was performed on the LightCycler480 (Roche) and amplification of specific PCR products was detected using the RT2 SYBR Green Fluor PCR Master Mix (Qiagen Catalog No.330510) according to the manufacturer's protocol. Amplification of miR-520g was performed using LightCycler96 (Roche) using the TaqMan Universal PCR Master Mix without amperase UNG and TaqMan miRNA primer assays (Life Technologies): miR-520g-3p (1121), and U6 snRNA. Forward and reverse primers for PDPN mRNA were used at a final concentration of 200 nM and all primers employed were cDNA specific and were synthesized by Integrated DNA Technologies – IDT. Primer combinations are shown in Table 1.

Primers

Gene	Primer forward (5′–3′)	Primer reverse (5′–3′)
PDPN	TCCTCGGGAGAGATAAATGCTGACT	CCGGAGAGGGAGGGTGCCCGAGCTT
GAPDH	GAAGGTGAAGGTCGGAGTCA	TTGAGGTCAATGAAGGGGTC
Beta Actin	CTCTTCCAGCCTTCCTTCCT	TGTTGGCGTACAGGTCTTTG

Blank and standard controls were run in parallel to verify amplification efficiency within each experiment. Within each run, a melting curve analysis was performed to confirm the specificity of amplification and lack of primer dimers. The $2^{-\Delta\Delta Ct}$ equation was applied to calculate the relative expression of genes of interest in the corresponding cell lines and the equation E: 10−1/slope to calculate the efficiency of the RQ-PCR (values averaged around 2.1) was used to validate the efficiency of PDPN primers. The mean Ct value of the parental cell line (U373 and U87) was used as the calibrator point and reference. Average expression relative to reference was plotted with error bars representing SEM[9].

Protein immunodetection – extended

For immunoblotting, the indicated cells were lysed and harvested using Laemmli Lysis-buffer with complete proteinase inhibitor cocktail (Roche Applied Science). Protein concentration was quantified using the micro BCA protein assay kit (ThermoScientific), and samples containing 25-50 µg of total protein were resolved on 12% gradient SDS-PAGE. After blotting, PVDF transfer membranes (G&E Amersham) were blocked with 5% skimmed milk (5% BSA for phospho-antibodies) and probed with the indicated antibodies , including: anti-PDPN (Abcam Catalog No.128994), anti-EGFR (CellSignaling Catalog No. 4267L), anti-pEGFR Y1068 (CellSignaling

Catalog No. 2234S), anti-pAKT S473 (CellSignaling Catalog No. 9271S/4060S), anti–H3K27me3 (CellSignaling Catalog No. 9733S), anti–CD63 (Abcam Catalog No. ab134045), anti-TF (American Diagnostica Sekisui Catalog No. 4509), anti-Flotillin 1 (BD Transduction Laboratories Catalog No. 610821), anti–CD81 (Abcam Catalog No. ab79559), anti-Syntenin (Abcam Catalog No. ab133267), anti-CD9 (Abcam Catalog No. ab2215), anti–β-actin (Sigma Catalog No. A5441) and anti-GAPDH (Sigma Catalog No. G8795). Signal was developed using ECL detection reagents (Amersham RPN2106/RPN2232) [10].

Mouse tumor models

For subcutaneous inoculation (s.c.), immunodeficient SCID mice (Charles River) harbouring the YFP transgene (YFP/SCID)[11] were injected with single cell suspensions of indicated glioma cell lines in serum free DMEM medium at 3 x 10^6 cells per mouse in 0.2 ml volume, in the left flank. Viability of cells was tested and exceeded 90% according to trypan blue exclusion assay. For intracranial inoculation (i.c), SCID/YFP transgenic mice were anaesthetized, surgically prepped, scull exposed, drilled and striatum stereotactically injected with 2 x 10^5 glioma cells per inoculum in 2 µl volume of serum free media, as described previously[1]. The site of injection was standardised using Stoelting Stereotaxic Injector at coordinates (AP = +0.5; ML = +1.5.; DV = -3.0) of bregma and sagittal sutures. For systemic EV injection, the indicated cells were cultured and EVs isolated from conditioned media as described earlier[10] and below. EV isolates were assessed for protein concentration using the BCA assay (Pierce Biotechnology, Rockford, IL) and the equivalent of 10 µg of intact EVs was injected into the tail vein (i.v.) of SCID/YFP mice. Within 15 minutes post injection, whole blood was collected via the inferior vena cava (IVC) and platelet poor plasma was isolated and stored until used[12]. All procedures involving animals were performed in accordance with the guidelines of the Canadian Council of Animal Care (CCAC) and the Animal Utilization

Protocols (AUP) approved by the Institutional Animal Care Committee (ACC) at MUHC RI and McGill University.

Blood collection

Collection of whole blood was performed in 3.8% sodium citrate and Apyrase from the inferior vena cava (IVC). A 150ul sample was taken for complete blood count (CBC; Diagnostic and Research Support Service (DRSS) Laboratory at the Comparative Medicine and Animal Resource Center, McGill), and the remaining sample was centrifuged at 1,500g for 10 minutes. Platelet-poor plasma (PPP) was collected and stored frozen at –80°C for further analysis.

EV isolation and analysis

To isolate EVs, conditioned medium (CM) was collected from cultured cells grown for 72 h in media containing 10% of EV-depleted FBS (Ultracentrifuged at 150,000g for 18 h at 4 °C). CM was centrifuged at 400g for 10 min, supernatant recentrifuged at 2,000g for 15 min, and remaining supernatant quickly poured off into clean tubes and passed through 0.8 μm pore-size filter. The resulting filtrate was concentrated using Amicon Ultra-15 Centrifugal Filter Unit (EMD Millipore, Billerica, MA) with 100,000 NMWL cut-off. The concentrate was mixed with 50% of iodixanol solution (Sigma, St. Louis, MO) and processed for density gradient ultracentrifugation at 200,000g for 2 h [10]. Fractions were serially collected, and their density was determined by measuring the absorbance at 340 nm of sample volumes taken from the individual fractions using an ELISA plate reader. Calculations were made in reference to a generated standard curve. Individual fractions were also analyzed for EV concentration and size distribution using nanoparticle tracking analysis (NTA) system (NS500, NanoSight Ltd., UK). Three recordings of 30 s at 37 °C were obtained and processed using NTA software (version 3.0). EVs from individual iodixanol fractions were

subsequently collected by ultracentrifugation, protein extraction performed, and concentration of EV proteins was quantified using the microBCA assay (Pierce Biotechnology, Rockford, IL). For nano-flow cytometry the conditioned medium from cells grown for 72 h was collected and processed for EVs as described previously [10]. The concentrated supernatant was analyzed by NTA and diluted with PBS to the concentration of 10^{11} particles/ml. EVs were incubated with indicated fluorophore-conjugated antibodies for 2 h at room temperature in the dark (anti-PDPN Alexa 488, Cat. No. 337006; anti-TF PE, Cat. No. 365203; anti-CD81 APC, Cat. No. 349509; anti-CD9 FITC, Cat. No. 312103, all from BioLegend). In order to clear out the excess and unbound antibodies, EVs were re-isolated from staining mixtures using qEV size exclusion chromatography (SEC) columns (Izon Science, UK) according to the manufacturer's instructions. The EV containing fractions (0.5 ml) were identified by NTA. Parallel isotype controls adequately matched with the corresponding antibodies were similarly processed and all samples were read using CytoFLEX flow cytometry system (Beckman Coulter, Pasadena, CA) equipped with 3 lasers (405, 488, and 640 nm wavelength) [10]. Data were acquired and analyzed using Cytexpert 2.0 software (Beckman Coulter). Microparticle (EV)-associated TF procoagulant activity (MP-TF PCA) was assessed using ZYMUPHEN MP-TF (Aniara, Cat. No. A521196) as per manufacturer's recommendations.

Immunostaining

Tumors were resected and preserved in fresh 4% paraformaldehyde (PFA). Tissue processing was performed in an automated tissue processor unit (Leica TP 1050 tissue processor), followed by paraffin embedding. Tissue blocks were sectioned using American Optical microtome into 5 μm thick sections mounted on pre-coated glass microscope slides[1]. Prior to staining, sections were de-waxed in Xylene, followed by re-hydration in a series of alcohol washes (95% to 50% ethanol). For hematoxylin and eosin (H&E) staining, rehydrated slides were washed and incubated in

Hematoxylin (1.5% Acid Solution, pH 2.5), then washed in water and dipped in the Blueing Solution. Partial dehydration (50% to 80% ethanol) was performed before proceeding to incubation in Eosin solution, which was then followed by three 5-minute washes in 99% ethanol and Xylene[1]. For immunostaining, first, antigen retrieval was performed using Vector Antigen Unmasking Solution heated to 95°C for 15 minutes. Primary antibodies used for these studies were specific for human PDPN (abcam Catalog No. 128994), mouse fibrin (abcam Catalog No. ab34269), mouse CD31 (R&D Catalog No. AF3628) and CD61 (Origene Catalog No. AP02622PU-N). Incubations with primary antibodies were carried out at 1:100 - 1:200 dilutions, overnight in a humidified chamber at 4°C. Thereafter, slides were washed three times in PBS (5 min each) and incubated with corresponding HRP-conjugated secondary antibodies, followed by final mounting in Vectastain Elite kit (PK-4006), ImPACT DAB (SK-4105), and VectaMount Mounting Medium (H-5000, Vector Labs, Burlington, ON, Canada). For fluorescent staining (Fibrin/CD31) secondary antibodies (Invitrogen donkey Anti-Rabbit Alexa Flour 488(Green) Catalog No. A21206, Invitrogen donkey Anti-Goat Alexa Flour 594 (Red) Catalog No. A32758) were incubated with tumor sections in the dark at 37°C for 1 hour. After a series of 5-minute PBS washes, slides were mounted with cover slips using Vectashield Hardset DAPI (Vector) glue, allowed to dry before being visualised as indicated[1]. Quantification of fibrin-occluded vessels was performed manually by the random selection of 7 vessel abundant fields within each slide and counting fibrin positive versus total vessels. Martius Scarlet Blue (MSB) staining was performed on tumor tissues, as per established institutional protocols (RIMUHC Pathology Labs). Representative MSB as well as CD61 stained slides were sent for whole slide scanning (Aperio ScansScope AT Turbo, Leica Biosystems). In each slide, seven representative, equal and random fields were used to quantify fibrin-occluded vessels.

Transmission electron microscopy (TEM) and immunogold staining

EVs were collected as described previously and washed using 0.1% sodium cacodylate buffer. Following EV sample preparation (ultracentrifugation, washing and fixation), charged TEM grids were laid over with 10 µl drops of fixed EVs and contact was maintained for 20 minutes. Grids were washed twice with 0.02 M glycine (5-10min each). For immunogold staining, grids were blocked by overlaying with 10µl drops of BCO blocking agent for 5 minutes followed by incubation with primary antibody (1:1 dilution) (anti-PDPN ab128994; anti-CD63 ab59479 - Abcam) overnight at 4 degrees. Grids were washed with DPBS 5 times (3min per wash), blocked again, and treated with 15µl drops of corresponding gold-conjugated secondary antibodies (1:20 dilution) for 30minutes. Grids were washed, again, dried and the negative staining was performed using 4% uranyl acetate, after which the grids were allowed to dry for 1hr. EV preparations were examined using FEI Tecnai 12 BioTwin 120 kV TEM (AMT XR80C CCD Camera System) at the Facility for Electron Microscopy Research (FEMR), McGill University.

ELISA

Commercially available enzyme-linked immunosorbent assay (ELISA) kits were used to estimate systemic levels of PDPN (LSBio, LS-F6466), PF4 (LSBio, LS-5404), D-dimer (LSBio, LS-F6179), TF (IMUBIND American Diagnostica Inc, 845) in plasma of tumor bearing mice (PDPN, PF-4, D-dimer) and tumor homogenates (D-dimer), as well as plasma samples from GBM patients cared for at the University of Virginia (UVA - D.S; N.K) (PDPN and TF ELISA). Patient plasma sample analyses were conducted anonymously under the approval of the institutional Research Ethics Board (REB, MUHC # 2019-5493). Assays were conducted according to the manufacturers' protocols in duplicates, and their sensitivities as reported by the manufacturers

were: 0.156 ng/ml for PDPN, 0.068 ng/ml for PF4, 243.7 pg/ml for D-dimer, and 10 pg/mL for TF. ELISA readings of OD were performed using TECAN Infinite 200 PRO multimode plate reader equipped with i-control™ software interface.

Platelet activation in the presence of GBM cells and respective EVs

To assess platelet activation in the presence of $PDPN^{high}$ vs $PDPN^{low}$ GBM cells, the respective U373P and U373vIII cells were cultured in 8 chamber Falcon Culture Slides. At 48-72 hours later, culture media was removed, and cells were washed three times with PBS. Platelets freshly extracted by differential centrifugation from blood of YFP-SCID mice in the presence of Apyrase (Millipore Sigma, Catalog No. A6237) in Tyrode's buffer and finally resuspended in pre-warmed PBS (37°C) were added on top of the cells and incubated for 10 min at 37°C. Following incubation, a fixative solution PAMFix (Platelet Solutions, Catalogue No. PSR-001) was added. Following fixation, chamber slides were spun down to allow the removal of the fixative and preparations were stained using monoclonal APC-conjugated anti-P-Selectin antibody (CD62-P/APC, Psel.KO2.3). Similarly, platelet activation by EVs derived from either U373P or U373vIII cells was assessed via the co-incubation of freshly isolated platelets with respective EVs for 30 minutes with mild shaking. Following co-incubation, preparations were fixed, spun at 2000g and stained with APC-conjugated anti-P-Selectin antibody. All preparations were visualized using Zeiss LSM 780 confocal microscope.

Single-Cell RNASeq

Raw Single-cell RNA-seq data for GSE57872[13] were obtained from the Sequence Read Archive (*SRA*) data base. The data were aligned using HISAT2 and the obtained counts were applied to scImpute for the imputation of dropout event values. The imputed dataset was then normalized to

obtain TPM (transcript per million) values, converted to logarithmic scale, and centred by subtracting the mean values of genes across samples. TCGA expression data for Glioblastoma[14] were downloaded as z-scores using the cBioPortal for Cancer Genomics[15]. Violin and TSNE plots were created in R environment using packages *ggplot2* and *Rtsne*, respectively. Expression data for EGFR and PDPN were scaled and used for k-means clustering of samples using *ComplexHeatmap* package from R/Bioconductor[16]. PDPN and Cluster signatures were identified by extracting top 50 feature genes from GSEA analysis as indicated by comparing groups of samples[17]. The roadmap plots were generated from an independent set of scRNAseq data as recently described [18].

TCGA Data analysis

TCGA expression data for Glioblastoma[14] were downloaded as z-scores using the cBioPortal for Cancer Genomics[15]. Expression data for EGFR and PDPN was scaled and used for k-means clustering of samples using the ComplexHeatmap package from R/Bioconductor[16].

Identification of gene expression signatures for EGFR/PDPN-based clusters

Cluster signatures were identified by extracting the top 50 positively and negatively associated feature genes using GSEA[17]. Briefly, for each cluster, GSEA was used to rank the genes in order of their differential expression, using the signal-to-noise metric, between the cluster and the rest of the samples. From this list, the top 50 (POS, positive, upregulated) and the bottom 50 (NEG, negative, downregulated) genes were extracted as the signature genes for the cluster analyzed. This process was repeated for each cluster in the RNA-seq data set.

Gene set enrichment analysis was also performed using GSEA, where each gene set (e.g. the POS signatures of a specific single-cell RNA-Seq cluster) was tested for its enrichment among up-regulated or down-regulated genes in another dataset (e.g. the TCGA bulk-tissue data) to identify the relationship between the EGFR/PDPN-based cell clusters and bulk tissue data.

Data analysis and statistics

Analysis of Pfister-46 GBM dataset was performed using the R2 Genomics Analysis and Visualization Platform and employed statistical one-way analysis of variance (ANOVA). TCGA dataset analysis for PDPN mRNA levels as function of IDH1 mutational status was performed using GlioVis Data Visualization Tools for Brain Tumor Datasets, which employed the paired t-test statistical analysis. Statistical analysis of platelet counts, ELISA experiments, as well as fibrin and CD61 positive blood vessel counts was done using ANOVA and Tukey's multiple-comparison post-test. A P value of <0.05 was used as a measure of significance of difference between groups. GraphPad Prism 6.0 (GraphPad Software, Inc., San Diego, CA) was used to perform the latter statistical analyses.

SUPPLEMENTARY RESULTS

Interrelationship between PDPN and EGFR in glioblastoma cell populations. Oncogenic activation of the EGFR signalling pathway was previously linked to dysregulation of GBM-related coagulome, including elevated expression of TF in glioma cell lines [19]. While EGFR is amplified, mutated (EGFRvIII), or upregulated in a subset of GBMs (classical, mesenchymal) the impact of these events on the emerging mediators of VTE, such as PDPN[20,21], has not been extensively

explored in clinical samples especially in view of cellular heterogeneity underlying GBM progression[13]. To explore the possible interrelationships between EGFR and PDPN expression at the cellular level we interrogated the single cell RNA-seq data set comprising subtype annotated GBM cell samples[13] (Fig. S2 and S3). We employed the K-means clustering approach focusing on PDPN and EGFR expression to audit single cell transcriptomes pooled from 5 different GBM tumors. This analysis predictably revealed the existence of four different tumor cell phenotypes, including: $PDPN^{low}/EGFR^{high}$ (Cluster 1), $PDPN^{high}/EGFR^{high}$ (Cluster 2), $PDPN^{low}/EGFR^{low}$ (Cluster 3), $PDPN^{high}/EGFR^{low}$ (Cluster 4) (Fig. S3a). To assess whether this reflects a random distribution of PDPN and EGFR, or a cellular pattern, we developed extended gene expression signatures by comparing the genome-wide gene expression profile of each cluster to remaining cells within the dataset (Table S1). Except for the $PDPN^{low}/EGFR^{low}$ cells (Cluster 3), which showed high number of antithetically common signature genes with the $PDPN^{high}/EGFR^{high}$ (Cluster 2) and $PDPN^{high}/EGFR^{low}$ cells (Cluster 4), other clusters showed little overlap in their signature genes (≤3 genes; Fig. S3b). In accordance with these findings, the expression profile of the obtained gene signature differentiated between the four clusters, with the $PDPN^{low}/EGFR^{low}$ cluster (Cluster 3) standing apart from the rest of the cells (Fig. S3c). Again, $PDPN^{high}$ cells were positively enriched for coagulation transcripts (Fig. S3d). Moreover, while $PDPN^{low}/EGFR^{high}$ GBM cells expressed elevated transcripts linked to cell signalling, proliferation and differentiation (OLIG1, DLL1), transcriptomes of their $PDPN^{high}/EGFR^{low}$ counterparts were enriched for regulators of hemostasis and inflammation (C1R, C1S, CLEC2B) (Table S1). These observations further suggest that enrichment or depletion for PDPN is not a random effect and points to the involvement of distinct transcriptional programs among GBM cell subpopulations.

We further clustered bulk tumor transcriptomes available through TCGA around PDPN and EGFR expression levels (Fig. S3e). This analysis revealed the existence of four tumour subgroups with distinct global phenotypes (Ph; Fig. S2), including: $EGFR^{low}/PDPN^{low}$ (Ph1), $EGFR^{low}/PDPN^{high}$ (Ph2), $EGFR^{high}/PDPN^{low}$ (Ph3) and $EGFR^{high}/PDPN^{low/intermediate}$ (Ph4). Interestingly, these phenotypes only partially overlap with TCGA mandated transcriptional subtypes[22] in that Ph4 subgroup is enriched for classical GBM, while Ph2 contains several mesenchymal tumors (Fig. S3e). This data also suggests that $PDPN^{low}/EGFR^{high}$ phenotype of single GBM cells observed earlier (Fig 2A, Cluster 1) may be enriched in Ph3 and Ph4 bulk tumour subsets, while $PDPN^{high}/EGFR^{low}$ (Fig. S3a; Cluster 4) cells may dominate the Ph2 GBM subgroup. If this were to be the case the respective tumours would be expected to be enriched for the expression of the aforementioned 50 single cell gene signatures (Table S1). To test this possibility, we performed GSEA to examine whether the top 50 positive gene signatures of each single cell cluster are enriched in the gene signature of whole GBM tumors (TCGA) with similar PDPN/EGFR expression pattern. This was, indeed, found to be the case (Fig. S3f). We therefore reasoned that a distinctive gene expression signatures of GBM cell populations with antithetical expression levels of EGFR and PDPN may suggest a mechanistic link between these two genes and impact coagulant profiles of the corresponding tumors.

Epigenome-impacting mutations of IDH1 oncogene down-regulate PDPN expression in glioma. While the influence of EGFR on PDPN may depend, at least in part, on the concomitant EZH2 activity, other mutant oncogenic drivers, such as IDH1 R132H, directly impact cellular epigenome[23,24]. IDH1 mutations drive a distinct (proneural-like) subset of GBMs, influence coagulant phenotype of glioma cells and their tissue factor (TF) levels[25] and are associated with low incidence of VTE[26]. Since PDPN is an important correlate and possibly an effector of VTE[20,21],

and has been linked to IDH1[27] we set out to test the levels of its transcript in subsets of GBM lesions expressing mutant or wild type IDH1[28] (Fig. S5a-f). GSEA revealed a negative association between IDH1 mutations and the expression of genes characterizing the $PDPN^{high}/EGFR^{low}$ GBM phenotype (Cluster 4) in the scRNA-seq dataset. These genes (and phenotype) positively correlated with the wild type IDH1 status in GBM (Fig. S5a). The differentials in PDPN transcript levels were also captured through the analysis of two independent data sets (Pfister-46 MAS5.0-u133p2 and TCGA) using the R2 and Glio-Vis Genomics Analysis and Visualization platforms, respectively (Fig. S5b and d). This influence correlates with DNA methylation levels affecting PDPN gene locus in IDH1 mutant tumours relative to their IDH1-wild type counterparts, as revealed by multiple probes specific for this genomic region (Fig. S5c). In contrast, the GBM subset expressing wild type IDH1 exhibits upregulated PDPN mRNA, including in an independent dataset (Fig. S5e, f). Thus, in glioma PDPN is a target of at least two different epigenetic mechanisms one operating at the level of DNA methylation and controlled by oncogenic IDH1, while the other is executed by chromatin modifications in association with EZH2 and modulated by oncogenic EGFR.

SUPPLEMENTARY LEGENDS - Figures and Tables

Supplementary Figure 1. PDPN expression correlates with mesenchymal differentiation roadmap of glioblastoma progenitors. **a.** Plot depicting the main differentiation roadmaps of glioblastoma cell subpopulations: PROG- progenitors, NEUR- neural, MES – mesenchymal, ASTRO – astrocytic, OLIG – oligodendrocytic, as revealed by single cell sequencing [18]; **b.** PDPN high expressing cells (yellow/orange/red cells) cluster in the region of MES GBM cells, with some

contribution of astrocytic and progenitor cells; **c.** EGFR expression is scattered between multiple cell populations with weak overlap with PDPN.

Supplementary Figure S2. The gene expression analysis workflow. To characterize PDPN expressing GBM cells and their EGFR status, the single cell GBM transcriptomes[13] were pooled and clustered around PDPN and EGFR expression patterns (Clusters 1-4). The gene expression signatures of these clusters were used to establish the phenotypes of PDPN expressing GBM cells and to interrogate their presence in bulk transcriptomes of TCGA dataset (Phenotypes 1-4). GSEA plots were developed to compare the PDPN phenotypes (see text).

Supplementary Figure S3. Interrelationship between PDPN and EGFR in glioblastoma cell populations. **a.** K-means clustering of single cells from five GBM patient-derived tumors using the expression profiles of EGFR and PDPN. Each column represents one single cell, with the centered log2 transcript per million (TPM) EGFR and PDPN expression shown in the heatmap. The ID of the patient from which each cell is derived, as well as the subtype classification of each cell according to Patel et al. 2014[13] is also shown on the top of the graph. **b.** The extent of overlap between gene expression signatures of PDPN/EGFR-based single cell clusters. The first eight bars in the bar graph represent the number of unique genes of each cluster, whereas the remaining bars represent intersection size, with the intersecting clusters shown using the vertical lines that connect the cluster nodes. **c.** K-means clustering of GBM single cells based on the expression signatures of PDPN/EGFR-based single cell clusters. Cell cluster annotation corresponds to those represented in panel **a**. **d.** Gene Set Enrichment Analysis **(**GSEA) showing the expression distribution of Hallmark Coagulation genes in PDPN/EGFR-based single cell clusters. In each panel, the x-axis represents the genes, sorted by their differential expression between the indicated clusters and the rest of the cells. Vertical black lines represent the genes that belong to the Hallmark Coagulation

according to: [Molecular Signatures Database – Hallmark Coagulation; M5946]. The curve represents the GSEA running enrichment score (ES). **e.** K-means clustering of TCGA bulk glioblastoma samples using centered normalized expression of EGFR and PDPN (z-score). The four sample clusters are referred to as molecular phenotypes: $EGFR^{low}/PDPN^{low}$ (Ph1), $EGFR^{low}/PDPN^{high}$ (Ph2), $EGFR^{high}/PDPN^{low}$ (Ph3) and $EGFR^{high}/PDPN^{low/intermediate}$ (Ph4). **f.** GSEA enrichment score (ES) of the positive gene signature of each cell cluster (rows) across the TCGA molecular phenotypes (columns). Each ES represents the enrichment of the positive gene signature of a cell cluster (Single cell dataset; C1-C4) among genes that are up-regulated in a given TCGA molecular phenotype (Ph1-Ph4) (red) or down-regulated (blue).

Supplementary Figure S4. Analysis of PDPN expression in GBM cells. **a.** Expression of PDPN transcript in the single cell GBM dataset[13] was compared between cells with verified EGFRvIII mutations and with wild type EGFR gene. While due to small numbers of datapoints the results are statistically inconclusive, of interest is a trend for lower PDPN expression in EGFRvIII mutant cells. **b.** Restoration of miR-520g expression (RT-PCR) from the methylated locus in U373vIII cells following treatment with 5 Azacytidine (Aza) documents effectiveness of treatment. Under identical conditions PDPN expression remained unchanged (Fig. 3**c**). **c.** Quantification of western blots from Fig. 3ab, depicting the effects of dacomitinib and pictilisib on PDPN and AKT activity. **d.** PDPN protein expression under exposure to EZH2 inhibitor (UNC1999) and EGFR inhibitor (dacomitinib), quantification of the western blot from Fig. 3f; Two-way ANOVA, $P<0.0001$.

Supplementary Figure S5. IDH1 mutation correlates with epigenetic silencing of the PDPN gene in glioma. **a**. GSEA analysis associates the signature of PDPN expressing cells (cluster 4) with the wild type and not mutant IDH1 gene in the single cell GBM dataset [13]. **b.** Independent dataset analysis of bulk GBM samples (Pfister-46-MAS5.0-u133p2 - GSE36245) suggests lower

PDPN expression in IDH1 mutant *versus* IDH1 wild-type tumors. **c.** Preferentially methylated PDPN gene locus in IDH1 mutant bulk glioblastoma samples (TCGA; x-axis) as detected using multiple independent probes (y axis). **d.** Independent analysis of TCGA bulk GBM samples using GlioVis platform indicates downregulation of PDPN transcript in tumors with mutant IDH1. **e.** Independent cohort of high-grade glioma (HGG) samples (Jabado - internal dataset[29-31]) reveals increased PDPN TSS200 locus methylation in IDH1 R132H mutant tumors and its reduced methylation in IDH1 wild type (IDH1-WT) tumors; color denotes different probes (bottom box). **f.** Corresponding PDPN mRNA expression (as in **e**) shows increased levels of PDPN transcript in IDH1 wild type brain tumors compared to IDH1mutant ones.

Supplementary Figure S6. Circulating tissue factor in plasma of glioma patients. ELISA analysis for TF antigen reveals considerable variability. Baseline – blood draw prior to treatment at diagnosis; PreMC1-5 – blood draws on the successive follow ups.

Supplementary Figure S7. PDPN expression, EV-mediated PDPN emission and platelet activation by glioma cells. **a.** GSEA plots depicting an inverse correlation between PDPN-associated gene expression signature and EZH2 target genes in single cell GBM data set (Patel et al 2014 [13]; see Fig. 1). **b.** Co-expression of PDPN and CD63 on U373PT glioma cell derived EVs – immunogold staining and electron microscopy (see Fig. 5; N=2). **c.** PDPN-expressing (U373P) and non-expressing (U373vIII) cells (left panels) and their EVs (middle panels) exhibit differential ability to trigger P-selectin exposure (red) by fluorescent mouse platelets (green). Platelets were isolated form mice harboring YFP transgene and incubated with intact cancer cells (left panel), their EVs (right panel) or controls (right panels); only PDPN-expressing U373P cells efficiently triggered P-selectin exposure and platelet activation (compare Fig. 6; N=2).

Supplementary Figure S8. Tumor burden, RBC counts, and microparticle-TF procoagulant activity (MP-TF PCA) in the U373P-related models of glioblastoma. **a.** Plot of tumor volumes of U373-PT, U373vIII, and U373TF G11-PT xenografts highlighting comparable tumor volumes among conditions. **b.** RBC counts plot of all tumor-bearing mice depicting counts comparable among conditions and insignificantly different from those of control tumor-free mice. **c.** MP-TF PCA assessment in EVs isolated from U373, U373vIII and U373TF G11 cells (A431 EVs used as positive control). **d.** MP-TF PCA assessment in peroxide (20μM) treated EVs isolated from U373, U373vIII and U373TF G11 cells; peroxide was used to cause TF decryption [32]. **e**. Assessment of MP-TF PCA in conditioned unfractionated media from U373P, U373vIII and U373TF-G11 cells. **e.** Assessment of TF PCA in soluble fraction of conditioned media. Amicon concentration column flow-through fraction following EV concentration step was assayed for U373P, U373vIII and U373TF G11 cells conditioned media. Independent repeats (c-e) N = 3; designations: ns – non-significant, P value: ** - 0.01; *** - 0.001; **** - 0.0001. ANOVA multiple comparison analysis.

Supplementary Figure S9. TF, MP-TF PCA and D-dimer levels in mice exposed to glioma tumors and EVs. Plasma of tumor-bearing and EV-injected mice as well as total D-dimer in whole tumor mass (TB) versus total plasma were assayed as indicated. **a**. TF levels and MP-TF PCA (**b**) in plasma of U373-PT, U373vIII, and U373TF G11-PT tumor-bearing mice. **c.** D-dimer levels in plasma of tumor-bearing mice**. d.** Total D-dimers in the whole tumor mass versus plasma of mice with the respective tumors (ELISA); ns – non-significant, P value: ** - 0.01; *** - 0.001;

**** - 0.0001; ANOVA multiple comparison analysis.

Supplementary Table S1. Top 50 gene signatures of clusters 1-4. Extended gene expression signatures for each cluster generated by comparing the genome-wide gene expression profile of that cluster to the rest of the cells within the single cell RNA-seq dataset[33].

Supplementary Table S2. Hallmark Coagulation gene set founding genes. List of genes constituting the HALLMARK COAGULATION gene set published by GSEA and retrieved from https://www.gseamsigdb.org/gsea/msigdb/cards/ *HALLMARK_COAGULATION*.

Supplementary Table S3. Hallmark Coagulation gene set ranked in order of expression in PDPN expressing cells (single cell RNAseq). List of genes constituting the HALLMARK COAGULATION gene set used in the GSEA protocol and retrieved from https://www.gseamsigdb.org/gsea/msigdb/cards/*HALLMARK_COAGULATION* listed according to the level of expression in PDPN expressing GBM cells in a descending order. Of note, not all genes of the Hallmark Coagulation are expressed at significant levels in PDPN expressing GBM cells. Interestingly, canonical coagulation factors such as F3, (tissue factor), PROS1 (protein S), or F8 (factor VIII) are ranked as 6th, 8th, and 37th highest expressed genes.

Supplementary Table S4. Hallmark Coagulation gene set ranked in order of expression in PDPN expressing GBM tumors (TCGA). List of genes constituting the HALLMARK COAGULATION gene set used in the GSEA protocol and retrieved from https://www.gseamsigdb.org/gsea/msigdb/cards/*HALLMARK_COAGULATION* listed according to the level of expression in PDPN expressing GBM tumors in a descending order. Of note, not all genes of the Hallmark Coagulation are expressed at significant levels in PDPN expressing GBM lesions. Interestingly, canonical hemostatic factors such as F3, (tissue factor), PROS1 (protein S),

or SERPINE1(PAI1) are ranked as 1st, 7th, and 16th highest expressed genes. This set contains mixed cellular populations and stroma and thereby differs from single cell data set in Table S3.

EXTENDED DISCUSSION

In this report we present evidence that oncogenic IDH1 and EGFR drivers control PDPN gene expression, at least in part, through the influence on the epigenome. For example, we observed that mutant IDH1R132H imposes a strongly hypermethylated state on the PDPN promoter DNA sequences driving down PDPN mRNA expression in a subset of high-grade brain tumours. This is in line with the known and wider effect of this mutation on the synthesis of an oncometabolite, D-2-hydroxyglutarate (D2HG), which inhibits cellular DNA demethylases thereby conferring a methylator phenotype (G-CIMP) upon a subsets of GBM[28] and acute myelogenous leukemia (AML)[33]. Notably, IDH1 mutant brain tumors are associated with proneural gene expression signature[22], better prognosis, minimal tumor microthrombosis and low VTE risk[26]. These tumours have recently been separated from the diagnosis of glioblastoma [34].

The clinical relevance of the nexus between oncogenic pathways and VTE risk in GBM patients is still unclear and at this time not considered actionable. However the very low incidence of VTE in patients with high grade glioma harbouring IDH1 mutation[35] along with low levels of TF[26] and PDPN expression[19] in these patients are thought provoking and worthy of functional analysis. In this regard developing biological criteria to distinguish subsets of GBM patients with different VTE risks is of great interest. While informative and striking in terms of thrombosis, IDH1 mutations are associated with a rare brain tumor subtype with distinct biology, hence recently separated from the general GBM diagnosis [34]. Therefore, explanations must still be sought for the

remaining GBM subgroups associated with high risk of thrombosis (25-30%)[26]. More individualized VTE prediction tools for these patients are badly needed.

Oncogenic EGFRvIII also exerts a silencing effect on PDPN albeit through a different epigenetic mechanism. We observed that EGFRvIII expression in glioma cell lines results in a profound reduction of PDPN mRNA and protein levels, which was not reversible by blockade of EGFR kinase activity by dacomitinib alone. However, inhibition of EZH2, the histone-lysine N-methyltransferase responsible for histone H3 repressive trimethylation (K27me3), partially and gradually rescued the PDPN expression in these cells, and this effect was further enhanced by co-treatment with EGFR kinase inhibitor. The profound effect of the epigenome on PDPN expression is illustrated by our observation that PDPN levels in glioma stem cells can be overridden by serum induced differentiation, which also results in upregulation of EGFR. Similar differentiation processes are likely to occur in GBM tissue *in vivo* resulting in the coexistence of different cellular populations with different PDPN (coagulant) profiles[36].

PDPN is a known target of several crucial signalling pathways in cancer, including AKT, as inferred from the inverse correlation between PDPN and PTEN tumour suppressor expression in glioma cell lines[37]. Such regulation could intersect with PDPN promoter methylation and hypoxia signalling, leading to elevated PDPN levels in some GBM cells[37]. This mechanism is of interest as mutant IDH1 was shown to inhibit AKT expression and activity[38] in addition to its effect on DNA methylation profile[39]. Indeed, our data suggesting a negative correlation between PDPN levels and IDH1R132H mutation may suggest some contribution of this mechanism.

The negative and kinase independent effect of the oncogenic EGFRvIII on PDPN expression in glioma cell lines was surprising in view of the inferences that could be made from the previously

reported upregulation of PDPN in EGFR expressing squamous cell carcinoma cells[40], along with the role of AKT (a suggested PDPN suppressor), or other downstream targets of EGFRvIII signaling[41]. It should be mentioned that U373vIII and U87vIII cells express no PTEN and that single cell GBM transcriptomes reveal the presence of both positive and negative correlations between PDPN and EGFR levels, of which our cellular models capture only the latter. Collectively, these results suggest an interplay between transforming mutations and the epigenetic control of PDPN expression along with the corresponding broader aspects of coagulant phenotypes associated with glioma cells.

Overall, the negative interrelationship between PDPN and EGFRvIII is surprising as the large proportion of IDH1 wild type GBM lesions express EGFR and of those several likely express PDPN and cause thrombosis. We postulate that heterogeneity of GBM lesions brings together cells with phenotypes driven by EGFR activity (possibly with PDPN low status) and those in which PDPN is expressed at high levels resulting in a net tumor and VTE promoting effects. Thus, two different functionalities (thrombosis and EGFR-driven growth) could be achieved by cooperation between GBM cell subpopulations [42-44].

It should also be noted that other coagulation factors, including TF, may exhibit different regulatory patterns in transfected glioma cell lines and at the single cell level in unmanipulated GBM cell populations. For example, while TF is consistently upregulated in glioma cell lines engineered to express EGFRvIII [6], its levels are often low in EGFR expressing glioma cells in intact tumours [19]. In our present study we used the cell lines merely as tools to observe the coagulant effects of glioma xenografts under the influence of TF and PDPN. However, the regulation of these and other factors in GBM is likely more complex and worthy of further investigation [19]. Indeed, epigenetic programs appear to override and modulate the hardwired

effects of oncogenic signalling [45] and may ultimately become a dominant force in driving coagulant phenotype and CAT in GBM.

We also present data to suggest that glioblastoma cells release PDPN (and TF) as cargo of exosome-like EVs *in vitro*, into the blood of tumor bearing mice and in GBM patients. Such EVs are endowed with a demonstrable procoagulant activity *in vivo,* which differs as a function of PDPN, TF or TF/PDPN content. PDPN-EVs may represent an attractive candidate for the long-postulated circulating coagulant that would provide a missing link between the procoagulant intracranial microenvironment in gliomas and the systemic impact of these tumors on the hemostatic system in the periphery[36,46-48].

We were puzzled by our observation that when co-expressed, PDPN and TF cooperate in driving microthrombosis. The relevance of these observation is enforced by the fact that in both single cell and bulk (TCGA) GBM transcriptomes the expression of high levels of PDPN coincided with the enrichment for Hallmark Coagulation gene expression signature [49] (Fig. 1de), in which TF was among the highest expressed genes in PDPN-positive GBM samples (Tabs. S3 and S4). It is tempting to speculate that this co-expression may create a potential for functional cooperation between PDPN and TF pathways in GBM tumors as suggested by our xenograft experiments.

The increasingly well documented association of PDPN with GBM-related CAT[20,50], if mechanistically validated, could contribute to a better stratification, monitoring and management of GBM patients at risk for VTE[48]. Like other thrombotic effectors[1], PDPN plays several important biological roles beyond hemostasis [51] and of possible relevance to the pathogenesis of GBM. Indeed, PDPN not only triggers signalling and activation of platelets *via* the CLEC2 receptor [21], but also serves as a signalling module in its own right, through the involvement in regulatory hubs

such as WNT/FZD complexes[52] and *via* interactions with multiple other proteins, including: CCL21, Galectin 8, CD9, CD44, and MMP14[51]. Consequently, PDPN has been implicated in cellular stemness, growth[37], vascular morphogenesis and lymphangiogenesis[51], effects that could be mediated by both direct cellular expression of this protein and, potentially, by its release as cargo of EVs[53]. While this is an attractive possibility recent studies suggest that PDPN correlates with but does not control GBM aggressiveness in experimental models [54].

PDPN is normally associated with lymphatic endothelium, podocytes and alveolar epithelium[55] and hence its activation in glioma cells with inflammatory signature and in other cancers[56] represents a biologically consequential anomaly. Our data suggest that PDPN expression could be turned on in PDPN-negative GBM cells by modulating the epigenome, which could add a cost of thrombosis to the use of epigenetic modifiers in cancer therapy.

We have earlier demonstrated that U373P-derived glioma xenografts shed EVs into the systemic circulation of tumor bearing mice[57]. Moreover, several aspects of this vesiculation process, including the composition of the EV proteome, are regulated by oncogenic driver genes, including EGFRvIII[10], with notable biological consequences[57]. For instance, in the case of U373vIII xenografts driven by oncogenic EGFRvIII the coagulant phenotype is mainly attributable to high TF expression[6], with largely undetectable expression of PDPN, in both cancer cells and EVs. This pathway of tumorigenesis was associated with predictably low PF4 levels, normal platelet counts and elevated D-dimers in blood. In contrast, in the EGFRvIII-independent tumorigenesis model (U373PT tumors) associated with low TF and high PDPN expression we observed a systemic activation of platelets (high PF4 release and thrombocytopenia), while D-dimers were comparable to those of tumour-free mice. When tumorigenic U373P cells were engineered to co-express PDPN and TF to mimic the coagulant complexity of some of the GBM tumors, the activation of platelets

still predominated systemically (high PF4, low platelets). This coagulant profile was also associated with elevated circulating D-dimers, and, interestingly, TF exacerbated microthrombosis locally, within the tumor mass. Overall, these observations highlight the possibility that different oncogenic pathways and microenvironmental influence may activate distinct coagulant processes within the same tumor type both locally and systemically.

Cancers, including GBM, are composed of rapidly evolving cellular lineages driven by parallel successions of genetic, epigenetic and regulatory events, all of which define the 'architecture' and apparent heterogeneity of constituent cellular populations[3]. We observed that in GBM this diversity translates into the expression pattern of key coagulant effector genes implicated in CAT, including TF, PDPN and several others [6]. Alignment of specific coagulant effectors, such as PDPN with identifiable pathways of oncogenic/epigenetic transformation may suggests the existence of unsuspected mechanistic links and non-random (targetable) pathways of CAT. We also suggest that these pathways may be different for microvascular thrombotic occlusion at the tumor site and macro-thrombosis in the peripheral circulation. In our GBM models the latter aspect is dominated by the activation of platelets in the presence of high levels of PDPN on cancer cells and PDPN-carrying tumor-derived (human) EVs in the peripheral circulation. Whether this reflects the association between PDPN and VTE in glioma patients requires further study.

REFERENCES FOR SUPPLEMENTARY TEXT

1. Magnus N, Garnier D, Meehan B, et al. Tissue factor expression provokes escape from tumor dormancy and leads to genomic alterations. *Proc Natl Acad Sci U S A*. 2014;111(9):3544-3549.
2. Spinelli C, Montermini L, Meehan B, et al. Molecular subtypes and differentiation programmes of glioma stem cells as determinants of extracellular vesicle profiles and endothelial cell-stimulating activities. *J Extracell Vesicles*. 2018;7(1):1490144.

3. Minata M, Audia A, Shi J, et al. Phenotypic Plasticity of Invasive Edge Glioma Stem-like Cells in Response to Ionizing Radiation. *Cell Rep*. 2019;26(7):1893-1905.e1897.
4. Mao P, Joshi K, Li J, et al. Mesenchymal glioma stem cells are maintained by activated glycolytic metabolism involving aldehyde dehydrogenase 1A3. *Proc Natl Acad Sci U S A*. 2013;110(21):8644-8649.
5. Micallef J, Taccone M, Mukherjee J, et al. Epidermal growth factor receptor variant III-induced glioma invasion is mediated through myristoylated alanine-rich protein kinase C substrate overexpression. *Cancer Res*. 2009;69(19):7548-7556.
6. Magnus N, Garnier D, Rak J. Oncogenic epidermal growth factor receptor up-regulates multiple elements of the tissue factor signaling pathway in human glioma cells. *Blood*. 2010;116(5):815-818.
7. Albrektsen T, Sorensen BB, Hjorto GM, Fleckner J, Rao LV, Petersen LC. Transcriptional program induced by factor VIIa-tissue factor, PAR1 and PAR2 in MDA-MB-231 cells. *J Thromb Haemost*. 2007;5(8):1588-1597.
8. D'Asti E, Huang A, Kool M, et al. Tissue Factor Regulation by miR-520g in Primitive Neuronal Brain Tumor Cells: A Possible Link between Oncomirs and the Vascular Tumor Microenvironment. *Am J Pathol*. 2016;186(2):446-459.
9. Livak KJ, Schmittgen TD. Analysis of relative gene expression data using real-time quantitative PCR and the 2(-Delta Delta C(T)) Method. *Methods*. 2001;25(4):402-408.
10. Choi D, Montermini L, Kim DK, Meehan B, Roth FP, Rak J. The Impact of Oncogenic EGFRvIII on the Proteome of Extracellular Vesicles Released from Glioblastoma Cells. *Mol Cell Proteomics*. 2018;17(10):1948-1964.
11. Yu J, May L, Milsom C, et al. Contribution of host-derived tissue factor to tumor neovascularization. *Arterioscler Thromb Vasc Biol*. 2008;28(11):1975-1981.
12. Chennakrishnaiah S, Meehan B, D'Asti E, et al. Leukocytes as a reservoir of circulating oncogenic DNA and regulatory targets of tumor-derived extracellular vesicles. *J Thromb Haemost*. 2018;16(9):1800-1813.
13. Patel AP, Tirosh I, Trombetta JJ, et al. Single-cell RNA-seq highlights intratumoral heterogeneity in primary glioblastoma. *Science*. 2014;%20;344(6190):1396-1401.
14. Brennan CW, Verhaak RG, McKenna A, et al. The somatic genomic landscape of glioblastoma. *Cell*. 2013;155(2):462-477.
15. Gao J, Aksoy BA, Dogrusoz U, et al. Integrative analysis of complex cancer genomics and clinical profiles using the cBioPortal. *Sci Signal*. 2013;6(269):pl1.
16. Gu Z, Eils R, Schlesner M. Complex heatmaps reveal patterns and correlations in multidimensional genomic data. *Bioinformatics*. 2016;32(18):2847-2849.
17. Subramanian A, Tamayo P, Mootha VK, et al. Gene set enrichment analysis: a knowledge-based approach for interpreting genome-wide expression profiles. *Proc Natl Acad Sci U S A*. 2005;102(43):15545-15550.
18. Couturier CP, Ayyadhury S, Le PU, et al. Single-cell RNA-seq reveals that glioblastoma recapitulates a normal neurodevelopmental hierarchy. *Nat Commun*. 2020;11(1):3406.
19. Tawil N, Bassawon R, Rak J. Oncogenes and Clotting Factors: The Emerging Role of Tumor Cell Genome and Epigenome in Cancer-Associated Thrombosis. *Semin Thromb Hemost*. 2019;45(4):373-384.
20. Riedl J, Preusser M, Nazari PM, et al. Podoplanin expression in primary brain tumors induces platelet aggregation and increases risk of venous thromboembolism. *Blood*. 2017;129(13):1831-1839.

21. Costa B, Eisemann T, Strelau J, et al. Intratumoral platelet aggregate formation in a murine preclinical glioma model depends on podoplanin expression on tumor cells. *Blood Adv*. 2019;3(7):1092-1102.
22. Verhaak RG, Hoadley KA, Purdom E, et al. Integrated genomic analysis identifies clinically relevant subtypes of glioblastoma characterized by abnormalities in PDGFRA, IDH1, EGFR, and NF1. *Cancer Cell*. 2010;%19;17(1):98-110.
23. Liu F, Wang L, Perna F, Nimer SD. Beyond transcription factors: how oncogenic signalling reshapes the epigenetic landscape. *Nat Rev Cancer*. 2016;16(6):359-372.
24. Sturm D, Bender S, Jones DT, et al. Paediatric and adult glioblastoma: multiform (epi)genomic culprits emerge. *Nat Rev Cancer*. 2014;14(2):92-107.
25. Unruh D, Mirkov S, Wray B, et al. Methylation-dependent Tissue Factor Suppression Contributes to the Reduced Malignancy of IDH1-mutant Gliomas. *Clin Cancer Res*. 2019;25(2):747-759.
26. Unruh D, Schwarze SR, Khoury L, et al. Mutant IDH1 and thrombosis in gliomas. *Acta Neuropathol*. 2016;132(6):917-930.
27. Sun C, Xiao L, Zhao Y, et al. Wild-Type IDH1 and Mutant IDH1 Opposingly Regulate Podoplanin Expression in Glioma. *Transl Oncol*. 2020;13(4):100758.
28. Reifenberger G, Wirsching HG, Knobbe-Thomsen CB, Weller M. Advances in the molecular genetics of gliomas - implications for classification and therapy. *Nat Rev Clin Oncol*. 2017;14(7):434-452.
29. Fontebasso AM, Papillon-Cavanagh S, Schwartzentruber J, et al. Recurrent somatic mutations in ACVR1 in pediatric midline high-grade astrocytoma. *Nat Genet*. 2014;46(5):462-466.
30. Krug B, De Jay N, Harutyunyan AS, et al. Pervasive H3K27 Acetylation Leads to ERV Expression and a Therapeutic Vulnerability in H3K27M Gliomas. *Cancer Cell*. 2019;35(5):782-797.e788.
31. Harutyunyan AS, Krug B, Chen H, et al. H3K27M induces defective chromatin spread of PRC2-mediated repressive H3K27me2/me3 and is essential for glioma tumorigenesis. *Nat Commun*. 2019;10(1):1262.
32. Bach RR. Tissue factor encryption. *Arterioscler Thromb Vasc Biol*. 2006;26(3):456-461.
33. Shih AH, Abdel-Wahab O, Patel JP, Levine RL. The role of mutations in epigenetic regulators in myeloid malignancies. *Nat Rev Cancer*. 2012;12(9):599-612.
34. Wen PY, Weller M, Lee EQ, et al. Glioblastoma in adults: a Society for Neuro-Oncology (SNO) and European Society of Neuro-Oncology (EANO) consensus review on current management and future directions. *Neuro Oncol*. 2020;22(8):1073-1113.
35. Diaz M, Jo J, Schiff D. P14.23 Risk of venous thromboembolism (VTE) in grade II-IV gliomas as a function of molecular subtype. *Neuro-Oncology*. 2019;21(Supplement_3):iii71-iii72.
36. Tawil N, Chennakrishnaiah S, Bassawon R, Johnson R, D'Asti E, Rak J. Single cell coagulomes as constituents of the oncogene-driven coagulant phenotype in brain tumours. *Thromb Res*. 2018;164 Suppl 1:S136-s142.
37. Peterziel H, Muller J, Danner A, et al. Expression of podoplanin in human astrocytic brain tumors is controlled by the PI3K-AKT-AP-1 signaling pathway and promoter methylation. *Neuro Oncol*. 2012;14(4):426-439.
38. Birner P, Pusch S, Christov C, et al. Mutant IDH1 inhibits PI3K/Akt signaling in human glioma. *Cancer*. 2014;120(16):2440-2447.

39. Turcan S, Rohle D, Goenka A, et al. IDH1 mutation is sufficient to establish the glioma hypermethylator phenotype. *Nature*. 2012;483(7390):479-483.
40. Fujii M, Honma M, Takahashi H, Ishida-Yamamoto A, Iizuka H. Intercellular contact augments epidermal growth factor receptor (EGFR) and signal transducer and activator of transcription 3 (STAT3)-activation which increases podoplanin-expression in order to promote squamous cell carcinoma motility. *Cell Signal*. 2013;25(4):760-765.
41. An Z, Aksoy O, Zheng T, Fan QW, Weiss WA. Epidermal growth factor receptor and EGFRvIII in glioblastoma: signaling pathways and targeted therapies. *Oncogene*. 2018;37(12):1561-1575.
42. Rak J. Is cancer stem cell a cell, or a multicellular unit capable of inducing angiogenesis? *Med Hypotheses*. 2006;66(3):601-604.
43. Wang X, Prager BC, Wu Q, et al. Reciprocal Signaling between Glioblastoma Stem Cells and Differentiated Tumor Cells Promotes Malignant Progression. *Cell Stem Cell*. 2018;22(4):514-528.e515.
44. Inda MM, Bonavia R, Mukasa A, et al. Tumor heterogeneity is an active process maintained by a mutant EGFR-induced cytokine circuit in glioblastoma. *Genes Dev*. 2010;24(16):1731-1745.
45. Neftel C, Laffy J, Filbin MG, et al. An Integrative Model of Cellular States, Plasticity, and Genetics for Glioblastoma. *Cell*. 2019;178(4):835-849.e821.
46. Falanga A, Marchetti M. Hemostatic biomarkers in cancer progression. *Thromb Res*. 2018;164 Suppl 1:S54-s61.
47. Geddings JE, Mackman N. Tumor-derived tissue factor-positive microparticles and venous thrombosis in cancer patients. *Blood*. 2013;122(11):1873-1880.
48. Hisada Y, Mackman N. Cancer-associated pathways and biomarkers of venous thrombosis. *Blood*. 2017;130(13):1499-1506.
49. Liberzon A, Birger C, Thorvaldsdóttir H, Ghandi M, Mesirov JP, Tamayo P. The Molecular Signatures Database (MSigDB) hallmark gene set collection. *Cell Syst*. 2015;1(6):417-425.
50. Mir Seyed Nazari P, Riedl J, Preusser M, et al. Combination of isocitrate dehydrogenase 1 (IDH1) mutation and podoplanin expression in brain tumors identifies patients at high or low risk of venous thromboembolism. *J Thromb Haemost*. 2018;16(6):1121-1127.
51. Quintanilla M, Montero-Montero L, Renart J, Martin-Villar E. Podoplanin in Inflammation and Cancer. *Int J Mol Sci*. 2019;20(3).
52. Bresson L, Faraldo MM, Di-Cicco A, Quintanilla M, Glukhova MA, Deugnier MA. Podoplanin regulates mammary stem cell function and tumorigenesis by potentiating Wnt/beta-catenin signaling. *Development*. 2018;145(4).
53. Carrasco-Ramirez P, Greening DW, Andres G, et al. Podoplanin is a component of extracellular vesicles that reprograms cell-derived exosomal proteins and modulates lymphatic vessel formation. *Oncotarget*. 2016;7(13):16070-16089.
54. Eisemann T, Costa B, Harter PN, et al. Podoplanin expression is a prognostic biomarker but may be dispensable for the malignancy of glioblastoma. *Neuro Oncol*. 2019;21(3):326-336.
55. Ugorski M, Dziegiel P, Suchanski J. Podoplanin - a small glycoprotein with many faces. *Am J Cancer Res*. 2016;6(2):370-386.
56. Kunita A, Baeriswyl V, Meda C, et al. Inflammatory Cytokines Induce Podoplanin Expression at the Tumor Invasive Front. *Am J Pathol*. 2018;188(5):1276-1288.

57. Al-Nedawi K, Meehan B, Micallef J, et al. Intercellular transfer of the oncogenic receptor EGFRvIII by microvesicles derived from tumour cells. *Nat Cell Biol*. 2008;10(5):619-624.